Short title;

IMPACT LOADING OF REINFORCED CONCRETE

MODEL PORTAL FRAMES

IMPACT LOADING OF REINFORCED CONCRETE MODEL PORTAL FRAMES

by

W.J. Dunn

A THESIS

Submitted to
The Faculty of Graduate Studies
and Research
in partial fulfillment of the requirements
for the degree of

MASTER OF ENGINEERING

Department of Civil Engineering
and Applied Mechanics,
McGill University,
Montreal, Canada.

June 1971.

IMPACT LOADING OF REINFORCED CONCRETE MODEL PORTAL FRAMES

W.J. Dunn

Department of Civil Engineering and Applied Mechanics.

M. Eng.

ABSTRACT

Four one-sixth scale model reinforced concrete portal frames were subjected to lateral impact and one to lateral static loading.

Response to repeated impact at the same load level and at sequentially increasing impact was studied. Results showed an increase in amplitude response and a decrease in natural frequency after repeated impacts at the same peak force. The successively higher impacts decreased the natural frequency and increased the logarithmic decrement of the frames free response. An increase in strength of the frames was evident during impact and all frames failed in a ductile manner. The elasto-plastic analysis, based on the static yield strength, showed a fair comparison with observations for small impacts but greatly overestimated deflections for larger impacts.

The experimental technique involved direct loading at beam level using a hydraulic force pulse system coupled to

the frame specimens with an electromagnet to separate the loading mechanism and the frame.

CHARGEMENT DYNAMIQUE DE MODELES REDUITS DE PORTIQUES EN BETON ARME

W.J. Dunn

Département de Génie Civil
et de Mécanique Appliquée.

M. Eng.
Juin 1971.

SOMMAIRE

Quatre modeles réduits de portiques en bétons armé, à l'échelle d'un sixième, ont été soumis à des charges latérales dynamiques. Un cinquième modèle fut sommis à une charge latérale statique. Leur comportement fut étudié sous charges dynamiques répetées de même intensité, puis d'intensité croissante.

Les résultats ont montré un accroissement de l'amplitude des déformations, et une réduction de la fréquence propre après plusieurs cycles de charge de même intensité. Les cycles successifs à charge croissante provoquèrent une diminution de la fréquence propre et un renforcement du décroissement logarithmique des amplitudes des vibrations propres.

On a observé un accroissement de la résistance des portiques sous l'effet des charges dynamiques; tous les portiques ont été soumis à une rupture ductile. Une analyse élasto-plastique fondée sur la limite d'élasticité statique des portiques a donneé une bonne comparison avec les résultats

expérimentaux pour de faibles charges mais a conduit à une surestimation des déformations pour des charges plus importantes.

Le technique expérimentale consista à charger les portiques du niveau de la poutre à l'aide d'un vérin hydraulique programmé, agissant par l'intermédiaire d'un électro-aimant. Ce dernier fut séparé pour l'obtension des vibrations propres des portiques.

ACKNOWLEDGEMENTS

The following research was financially supported by the Canada Emergency Measures Organization and directed by Professor J.O. McCutcheon, Chairman, Department of Civil Engineering and Applied Mechanics, to whom the writer is indebted for a research assistantship.

Many thanks to the professors, graduate students and technical staff of the Faculty of Engineering who gave of their time and talents to solve the experimental problems the writer would have been hopelessly overcome with himself.

Thanks to Mike and friends for their hand in building the frames.

The many authors and lecturers not referred to, but through whom the writer has gained his understanding of this topic are gratefully acknowledged.

Thanks to Mrs. Jackie Pass for typing this thesis from a lousy manuscript.

TABLE OF CONTENTS

TABLE OF CONTENTS (cont'd) Page

LIST OF FIGURES

LIST OF FIGURES (cont'd)

LIST OF PHOTOS

LIST OF TABLES

LIST OF SYMBOLS

A listing of programme notation is given in the appendix and symbols not listed below are defined directly after appearance in the text.

Tests are often designated with a letter, hyphon and number, e.g. A-23, the letter refers to the frame and the number to the test.

A_1 - Amplitude of the first positive (in direction of force pulse) deflection response peak after the linearized decay period of the force pulse dropped to zero.

A_n - Amplitude of the nth positive peak after A_1.

c - Effective viscous damping coefficient.

δ - Logarithmic decrement.

E_c - Modulus of elasticity of concrete.

f - Natural frequency of free vibration of the frame.

f'_c - Concrete compressive strength from 3" x 6" cylinders.

f'_t - Splitting tensile strength of concrete from 3" x 6" cylinders.

FI - Peak impulse load.

Hz - Cycles per second.

IT - Total impulse time.

LVDT - Linear variable differential transformer.

M - Mass.

LIST OF SYMBOLS (cont'd)

n	-	Number of cycles.
Q	-	Frame yield resistance.
RT	-	Force pulse rise time.
Ymax	-	Maximum lateral frame displacement.
Yres	-	Residual lateral frame displacement.

I. INTRODUCTION

1.1 Objectives

This investigation is a continuation of previous department studies into reinforced concrete structures subjected to static and dynamic loads. The present purpose is to study the behaviour of reinforced concrete portal frames under lateral impact load. Of particular interest are energy absorption, dynamic frame resistance and the suitability of the lumped mass, elasto-plastic viscously damped, mathematical model for determination of deflection response.

1.2 Experimental Procedure & Analysis of Results.

The experimental investigation involved building and testing five one-sixth scale model single bay reinforced concrete frames. The impact was applied as a direct lateral force pulse at beam level and was roughly triangular with approximately equal rise and decay times. In order to record the free transient response the force pulse apparatus and the frames were separated during impact. Separation was effected by means of an electromagnet link between the hydraulic ram of the force pulse apparatus and the frame specimens. The peak load of the impulse was determined by the electromagnetic force between pull-off plate and magnet.

1.3 Previous Work.

At McGill, Sader [17] tested and analysed twenty one-sixth scale model portal frames under vertical and varying horizontal static load. He concluded, "It is felt that the plastic analysis or the "Limit Design" gives a fairly good representation of collapse load", for these frames.

Using one of Sader's frames Liebich [1] tested six specimens (the same as those reported here except the steel was plain and non-heat treated) under direct impulsive loading at beam level. The Gilmore ram used to apply the impulse was rigidly attached to the specimen throughout the tests. Liebich observed, "The specimens tested dynamically exhibited greater peak loads than the ultimate strength of the static specimens, the stiffness of the frame decreased markedly with increasing number of cycles of loading and that the static and dynamic failure modes were similar and the frames showed a large ductility.

Watson [24] using small (six inch x 1-3/4 inch x 1-3/4 inch) unreinforced and reinforced mortar beams investigated their capacity to absorb energy when subjected to impact and static loads. Watson observed unreinforced beams "absorbed a constant 8% of impact energy until the impact energy reached 75 pounds-inches." At this level some of the beams were broken but those which survived a higher impact energy kept a constant 6.2 pounds-inches elastic energy absorbed." For the reinforced beams, "the elastic energy absorbed increases with increasing impact energy at all values used in the test. The existence of a limit as in the unreinforced beams is assumed since the percentage energy absorbed is decreasing.

Recent work outside McGill includes reinforced concrete portal frame model studies by Sabnis and White [8] reported in Section 3.1 and the following work by Takeda [3]. Takeda et al [3] investigated the response of five reinforced concrete columns (6" x 6" x 37.5") with masses attached at the top and full restraint at the bottom subjected to periodic and simulated earthquake motion at base level. Test results on these specimens were compared to an analytical study using "a realistic conceptual model which recognizes the continually varying stiffness and energy-absorbing characteristics of the structure." This model was based on the static force displacement relationships taking account of load level and history and involving a set of rules which were used to solve the equations of motion numerically. Takeda concludes "that the proposed force displacement relationships resulted in satisfactory agreement with the measured response at all levels of excitation with periodic and earthquake motions." Also, "with the hysteresis loops defined by the proposed force deflection relationship it was not necessary to invoke additional sources of energy absorption for a satisfactory prediction of the dynamic response."

II. APPARATUS

2.1 General

The problem of applying a prescribed impulse to the frame and separating the forcing system from the specimen, so that the free vibration response could be observed, was solved with an electromagnet link. The electromagnetic force holding the pull-off plate and the magnet together was controlled using a variable current supply to the magnet coil. When the pull from the force pulse apparatus exceeded the electromagnetic force the magnet and pull-off plate separated. Figure 1 shows the general arrangement of apparatus and details are shown on Figures 2 to 5 and Photos 1 to 12.

The structures laboratory Gilmore force pulse system was used to provide the tensile impulse force and is described in Reference 1. The pulse generator of the Gilmore apparatus was set to give a linearly rising voltage from zero to peak value (the first three voltage ramps of the pulse shaping circuits were given equal slopes) using a storage oscilloscope. The time of the fourth phase was adjusted to last for a few seconds so that when the frame and loading apparatus separated the electromagnet would move and stay away from the freely vibrating frame. It was found that Gilmore's system did not react fast enough so

NOTE
- WEIGHT OF ELECTROMAGNET SOCKET AND ADAPTER BOLT = 75.7 POUNDS.
- WEIGHT OF CAST IRON WEIGHTS & OTHER ATTACHMENTS = 629.3 POUNDS.

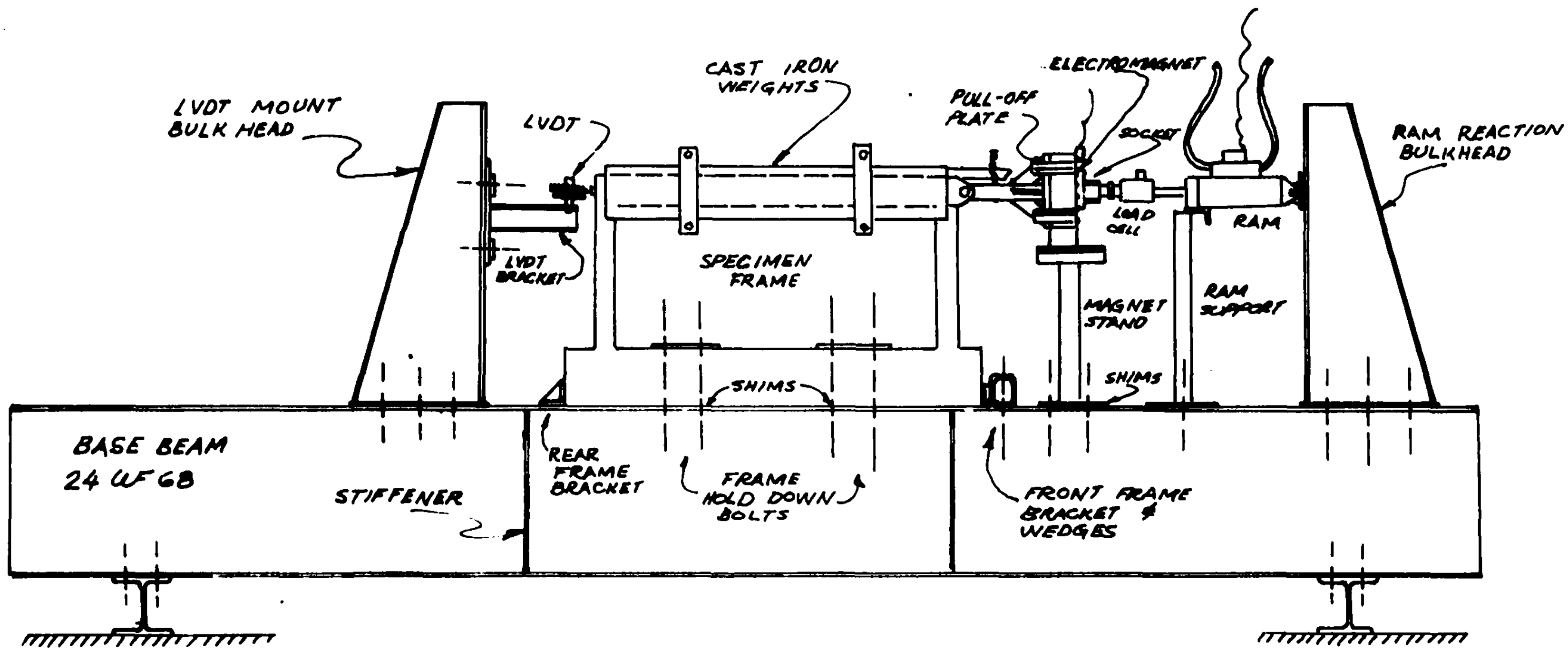

FIGURE 1 GENERAL ARRANGEMENT

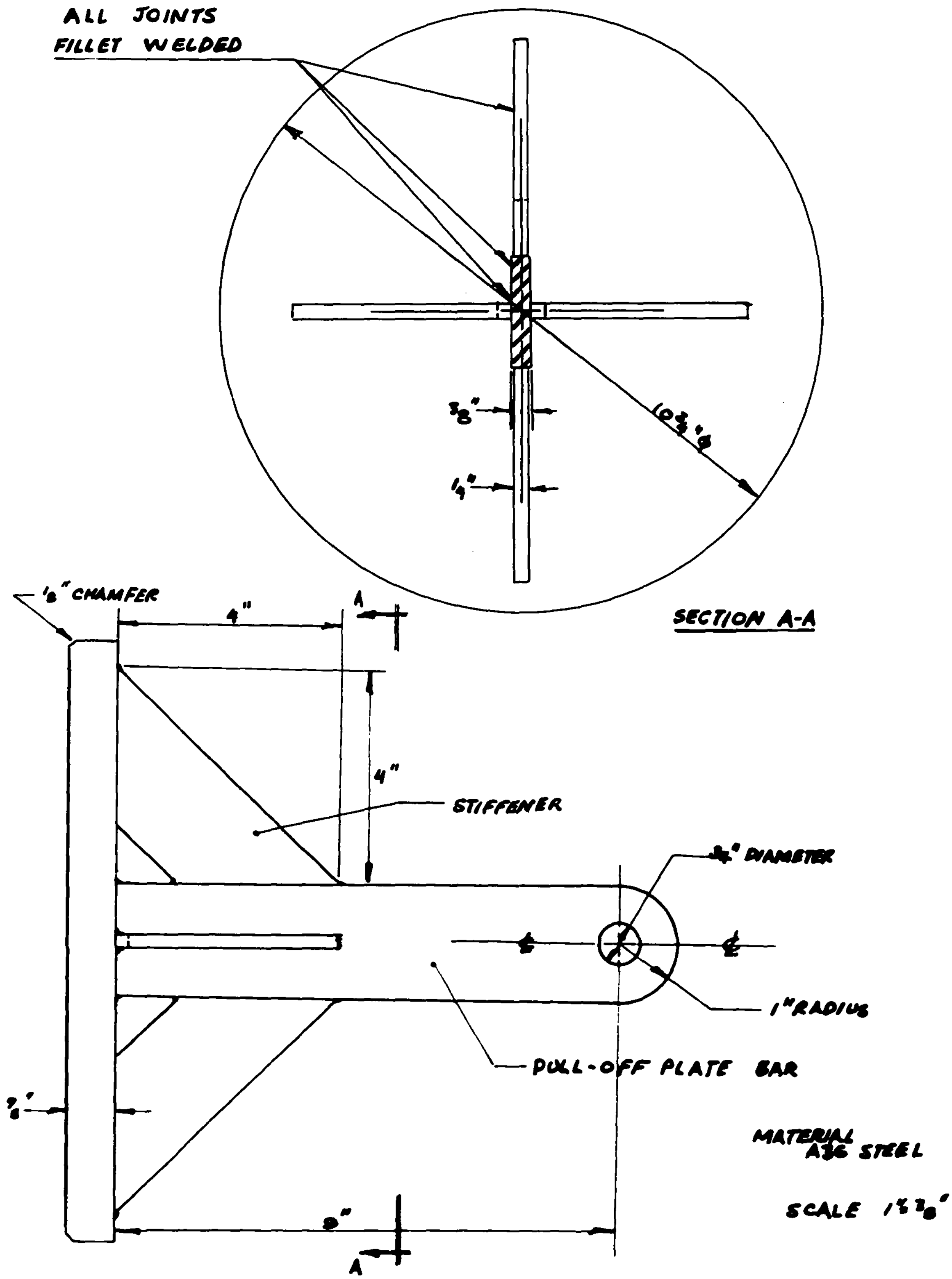

FIGURE 2 FRAME PULL-OFF PLATE DETAIL

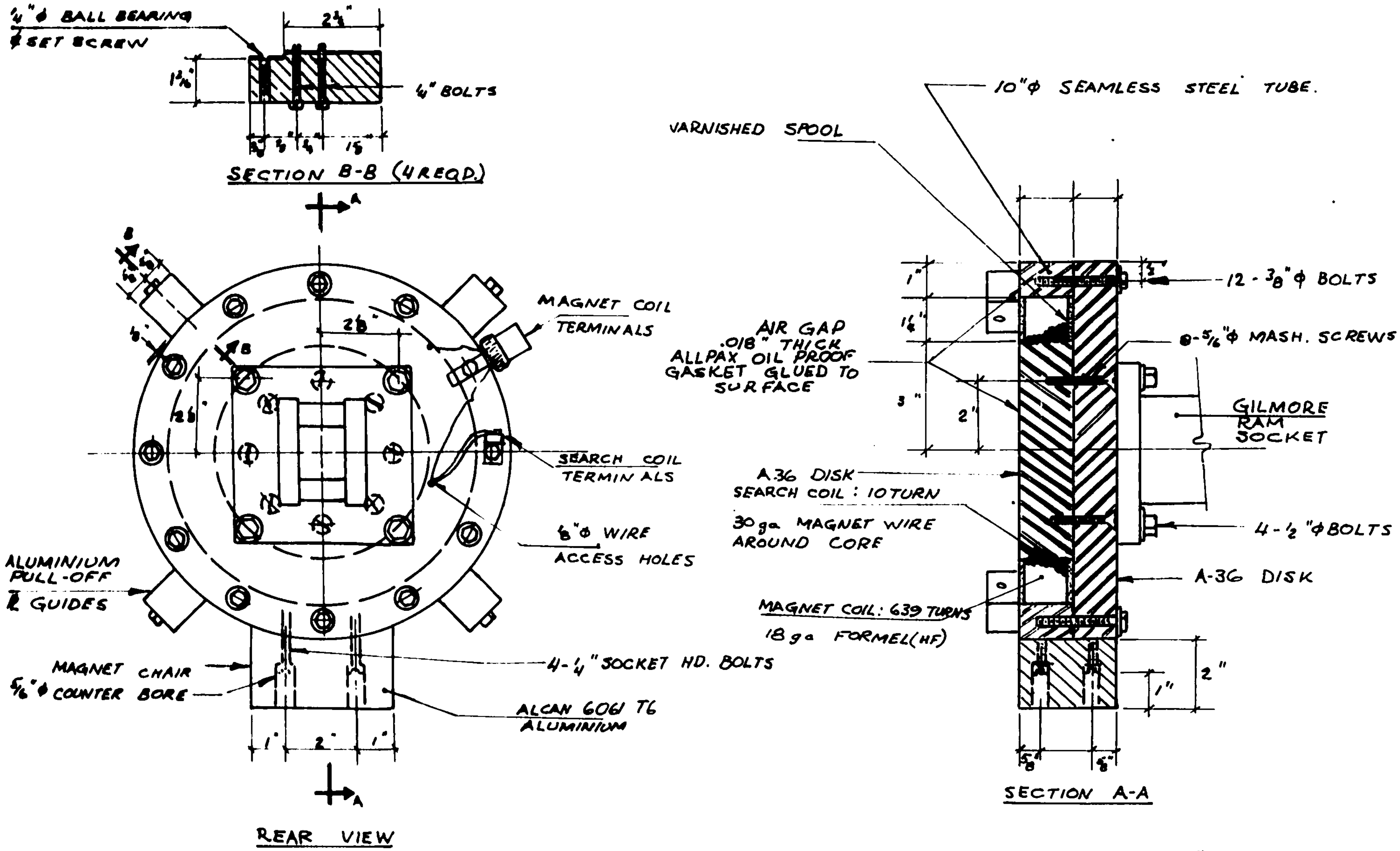

FIGURE 3 ELECTROMAGNET SCALE 1" = 1/4"

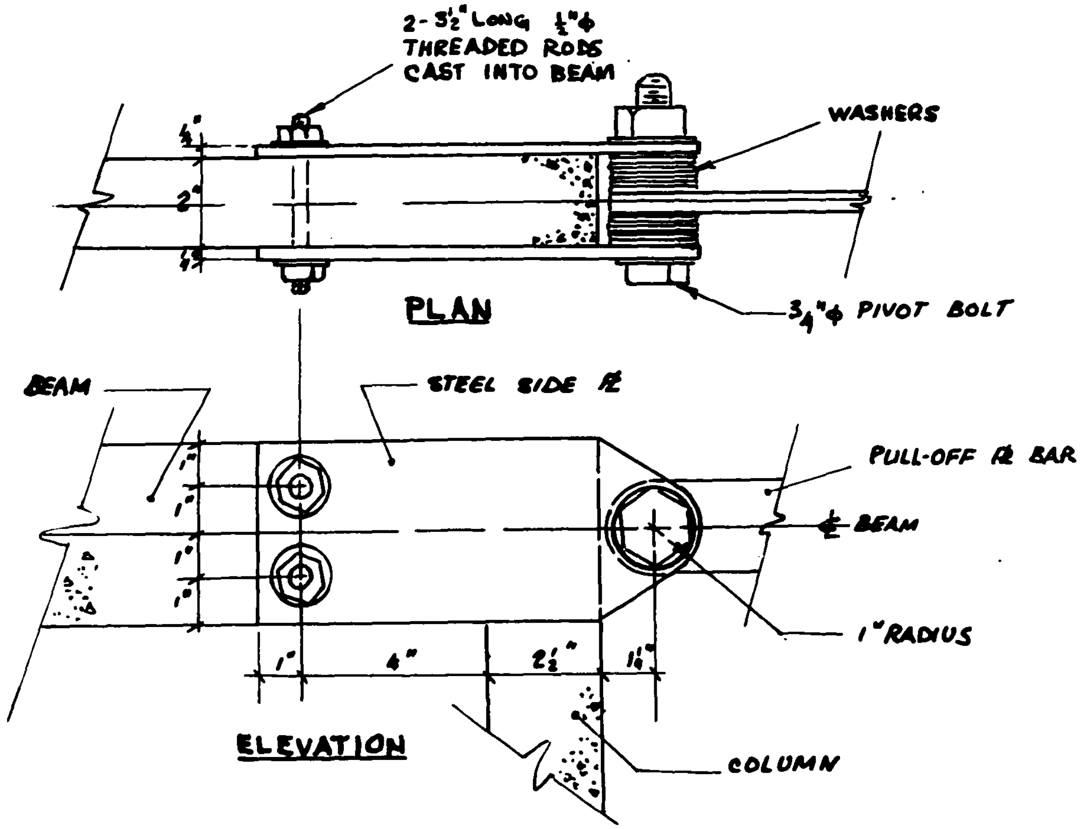

LATERAL FORCE TRANSFER DETAIL SCALE 1" = ¼"

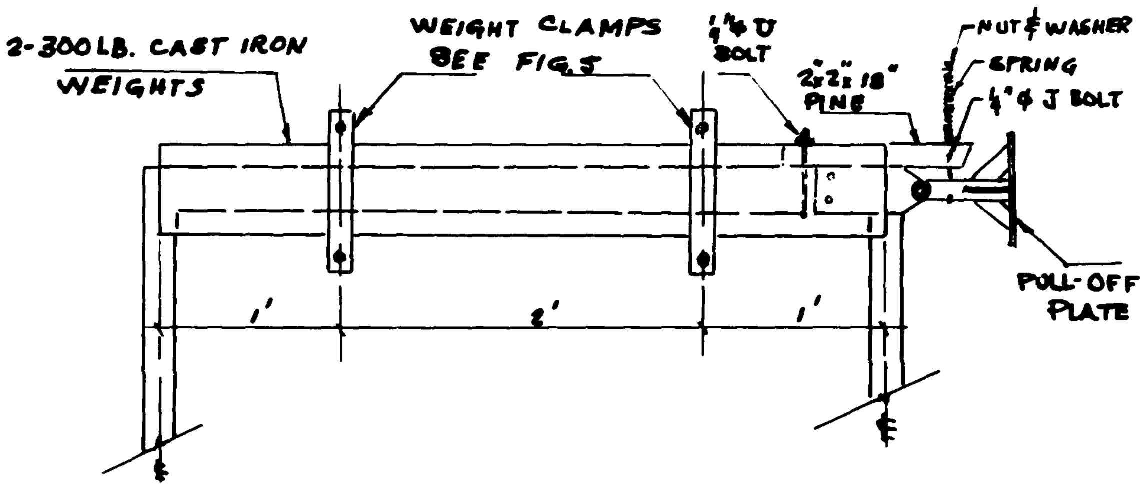

GENERAL ARRANGEMENT SCALE 1'-0" = 1"

FIGURE 4 FRAME ATTACHMENTS

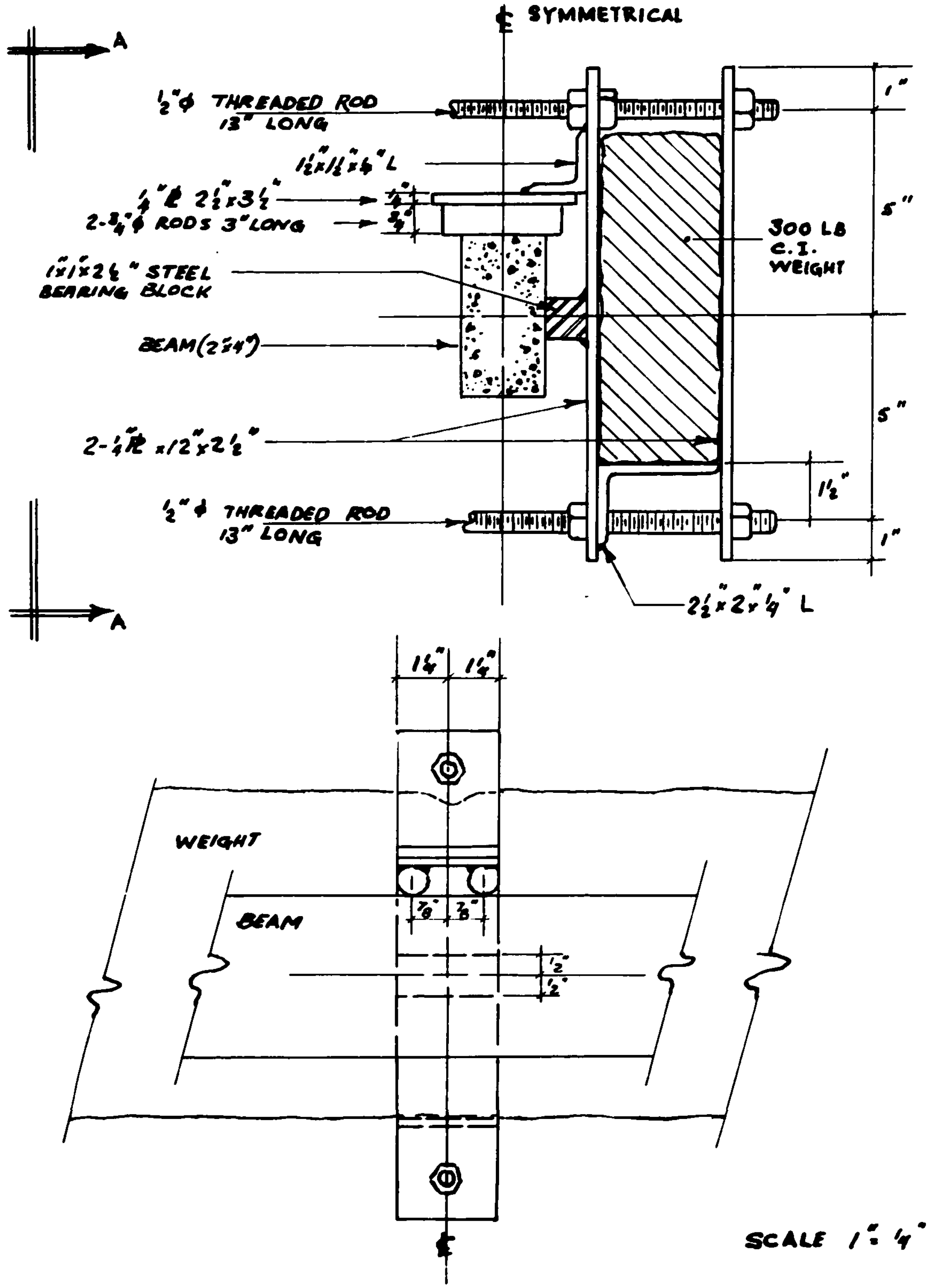

SECTION A-A

FIGURE 5 WEIGHT CLAMPS
(2 REQD)

PHOTO 1.
LVDT & MOUNTING BRACKET

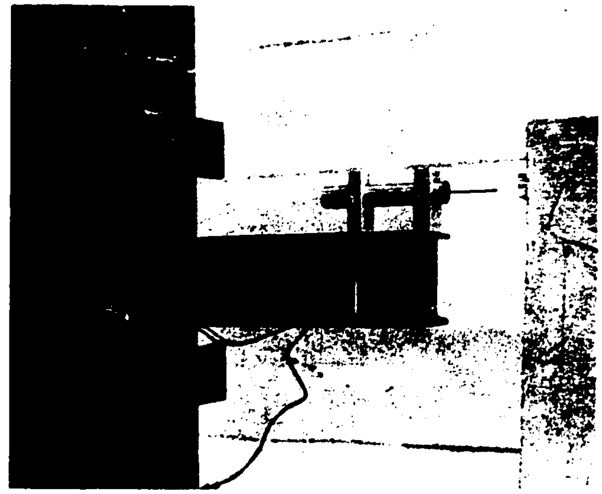

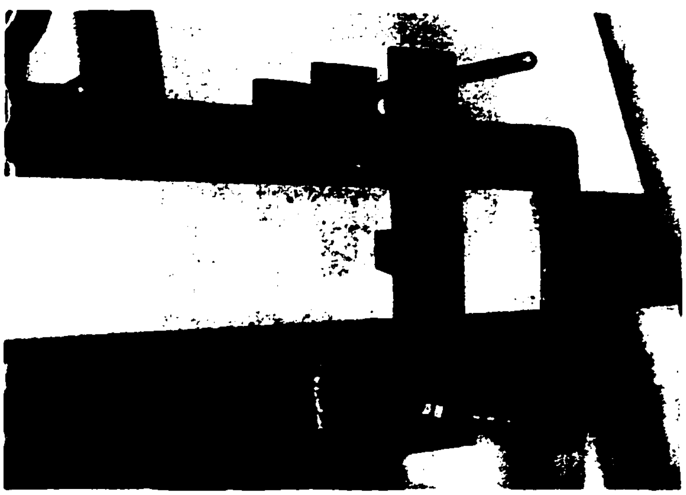

PHOTO 2.
CAST IRON WEIGHT & CLAMPS.

PHOTO 3
ELECTROMAGNET FRONT VIEW

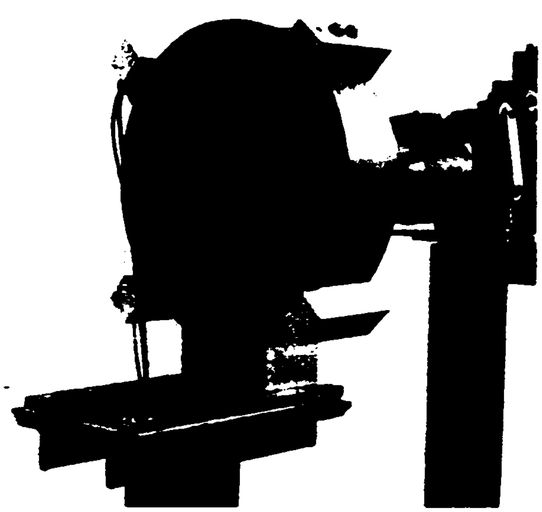

PHOTO 1.

LVDT & MOUNTING BRACKET

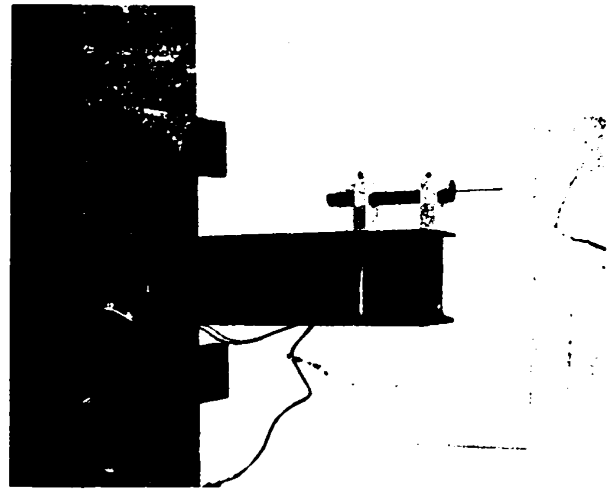

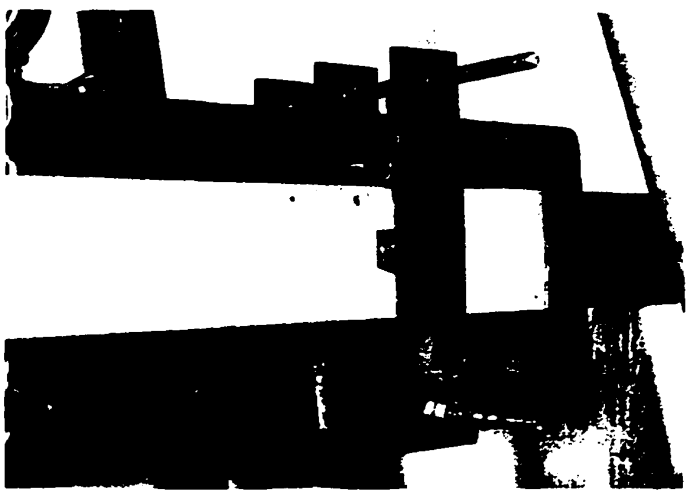

PHOTO 2.

CAST IRON WEIGHT & CLAMPS.

PHOTO 3

ELECTROMAGNET FRONT VIEW

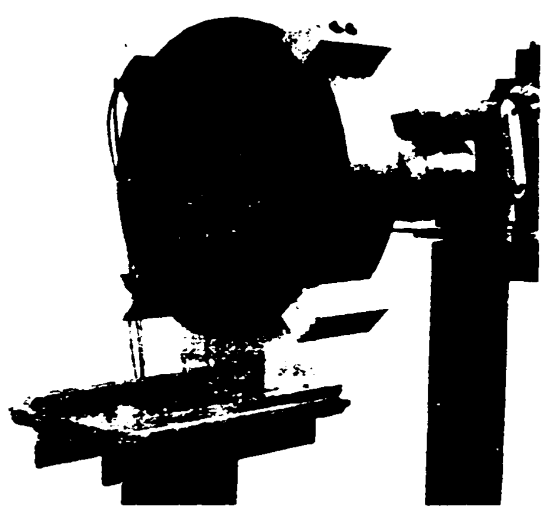

PHOTO 4.

HOIST FRAME & SPECIMEN PRIOR TO TESTING

PHOTO 5.

FRAME C & BASE BEAM HOLD DOWN CLAMPS

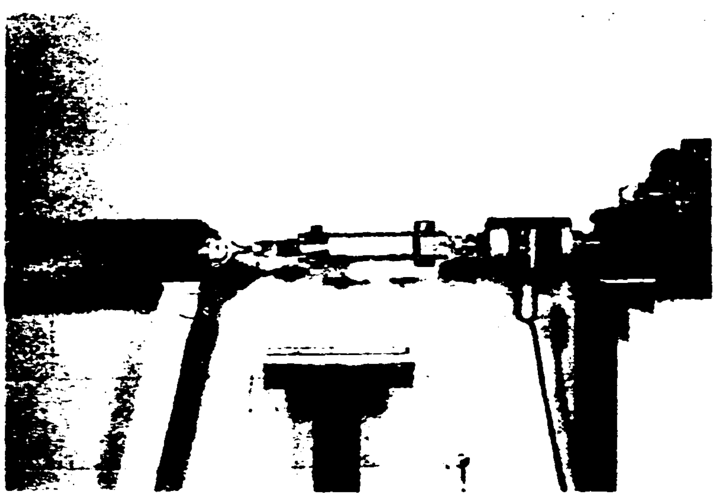

PHOTO 6.

STATIC TEST LOADING ARRANGEMENT.

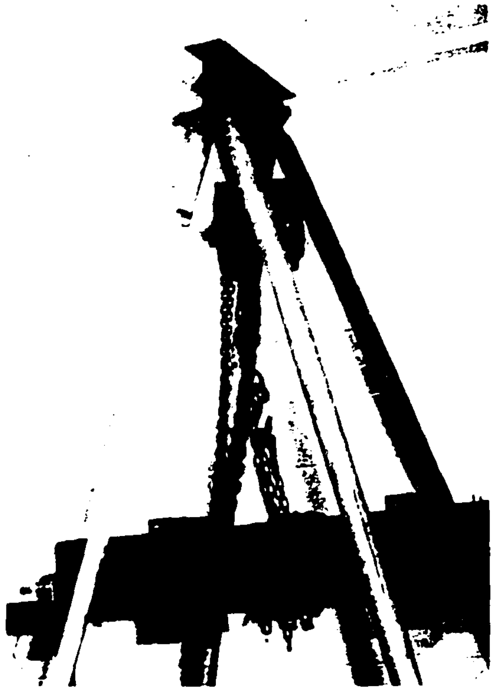

PHOTO 4.

HOIST FRAME & SPECIMEN PRIOR TO TESTING

PHOTO 5.

FRAME C & BASE BEAM HOLD DOWN CLAMPS

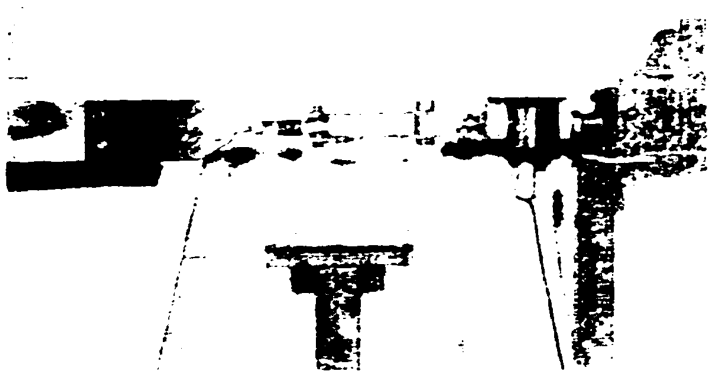

PHOTO 6.

STATIC TEST LOADING ARRANGEMENT.

PHOTO 7.

FRONT BASE BEAM
BRACKET & WEDGES

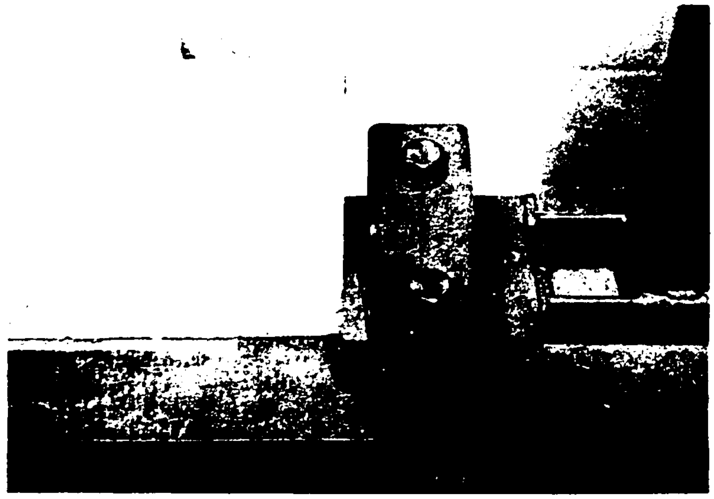

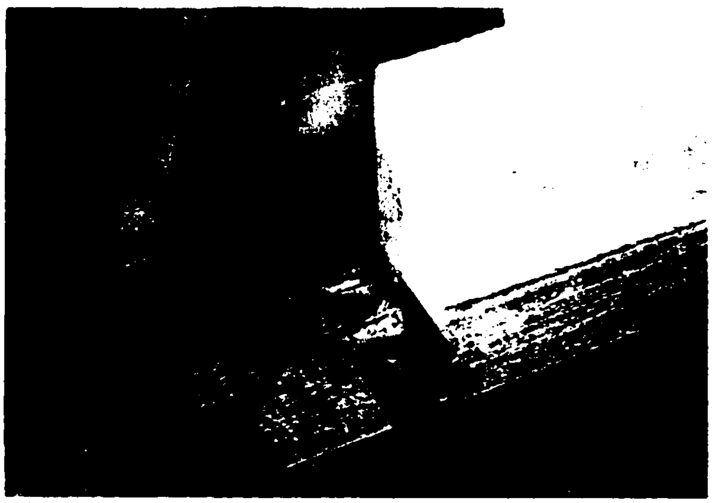

PHOTO 8

REAR BASE BEAM
BRACKET

PHOTO 9.

ELECTROMAGNET WITH
ACCELEROMETER.

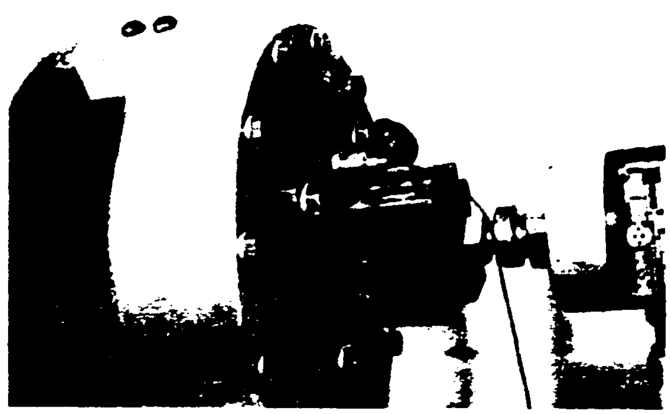

PHOTO 7.

FRONT BASE BEAM
BRACKET & WEDGES

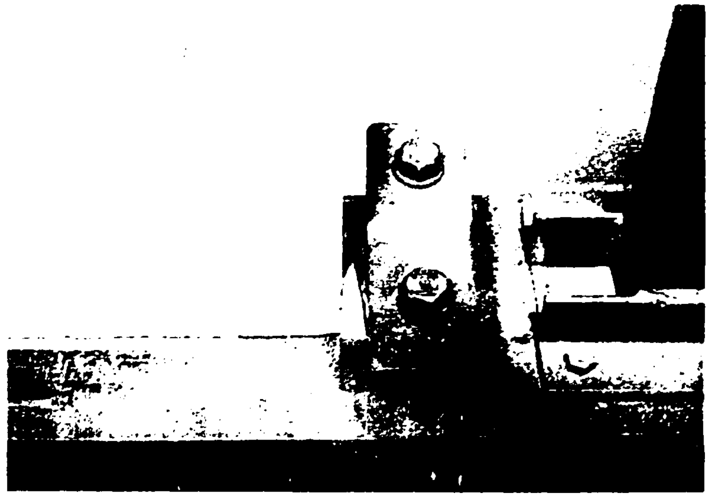

PHOTO 8

REAR BASE BEAM
BRACKET

PHOTO 9.

ELECTROMAGNET WITH
ACCELEROMETER.

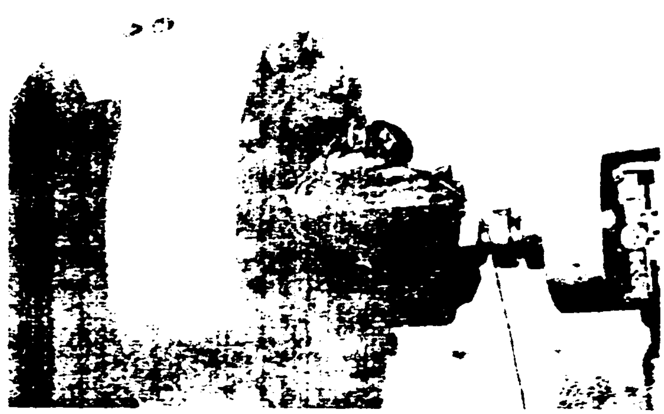

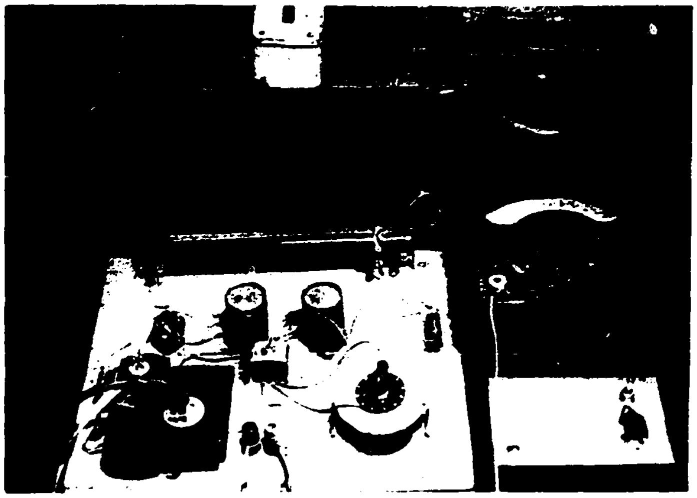

PHOTO 10.

ELECTROMAGNET
CURRENT CONTROL

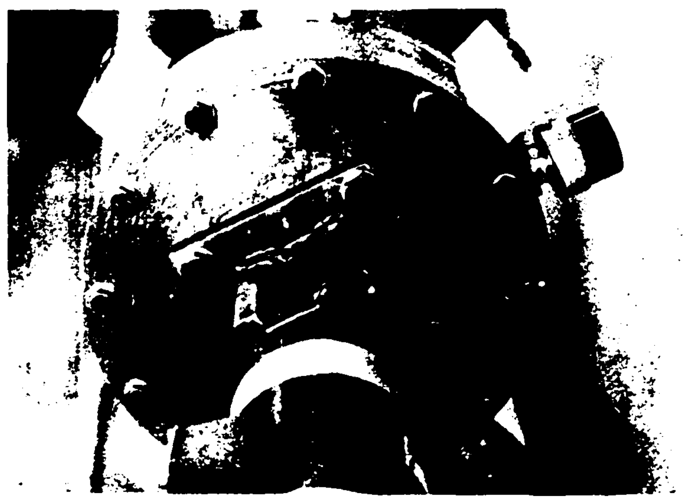

PHOTO 11.

ELECTROMAGNET REAR
VIEW.

PHOTO 12.

FRAME C AFTER
FINAL TEST

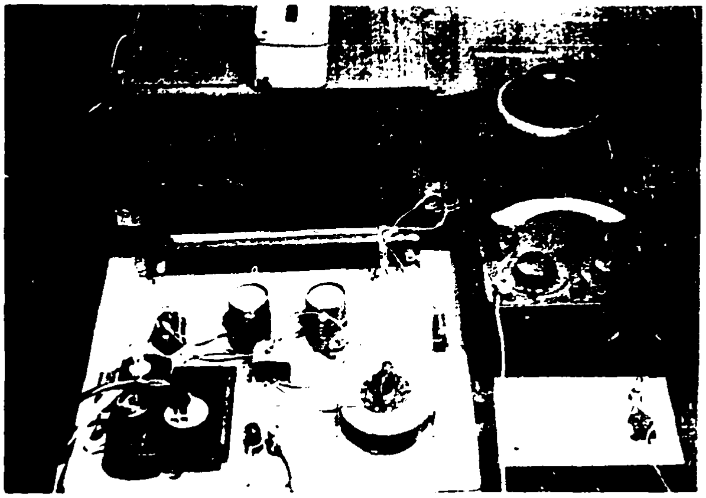

PHOTO 10.

ELECTROMAGNET CURRENT CONTROL

PHOTO 11.

ELECTROMAGNET REAR VIEW.

PHOTO 12.

FRAME C AFTER FINAL TEST

that the prescribed rate of increase of voltage from the pulse generator would result in an equivalent initial load rate.

The lateral deflection of the frame, measured at the centre of the beam, with respect to the base beam was monitored with a linear variable differential transformer, LVDT (Hewlett-Packard Co. type DCDT 1000),installed remote from the loaded end of the beam. The LVDT core was screwed into a plexiglas block which was in turn glued to the frame (see Photo 6.). Photo 1 shows the LVDT sleeve mounted to the adjustable bracket which was clamped to a bulkhead.

Prior to starting a test, the specimen was centered on the axis of the loading apparatus by plumbing from a wire strung between the two bulkheads in Figure 1. Shimming and adjusting the frame hold down bolts (Photo 5) served to align and bring the frame to the correct elevation. Before the hold down bolts were finally tightened the frame was firmly wedged between the rear (Photo 8) and front (Photo 7) brackets.

Mass,to simulate inertial forces, was provided by two 300 pound cast iron weights attached to the frame as shown in Figure 5 and Photo 2 (from which the near weight has been removed for clarity). Before a test the weights were loosely tied to a winch supported above the specimen on the hoist frame shown in Photo 4. This mechanism provided a fail safe device, but was never brought into service.

The loadcell monitor from the Gilmore console and the LVDT output were recorded on a Sanborn 320 dual channel recorder so that both the deflection and impulse signals would have the same time base. The Gilmore load cell

FIGURE 6 ELECTROMAGNET CALIBRATION

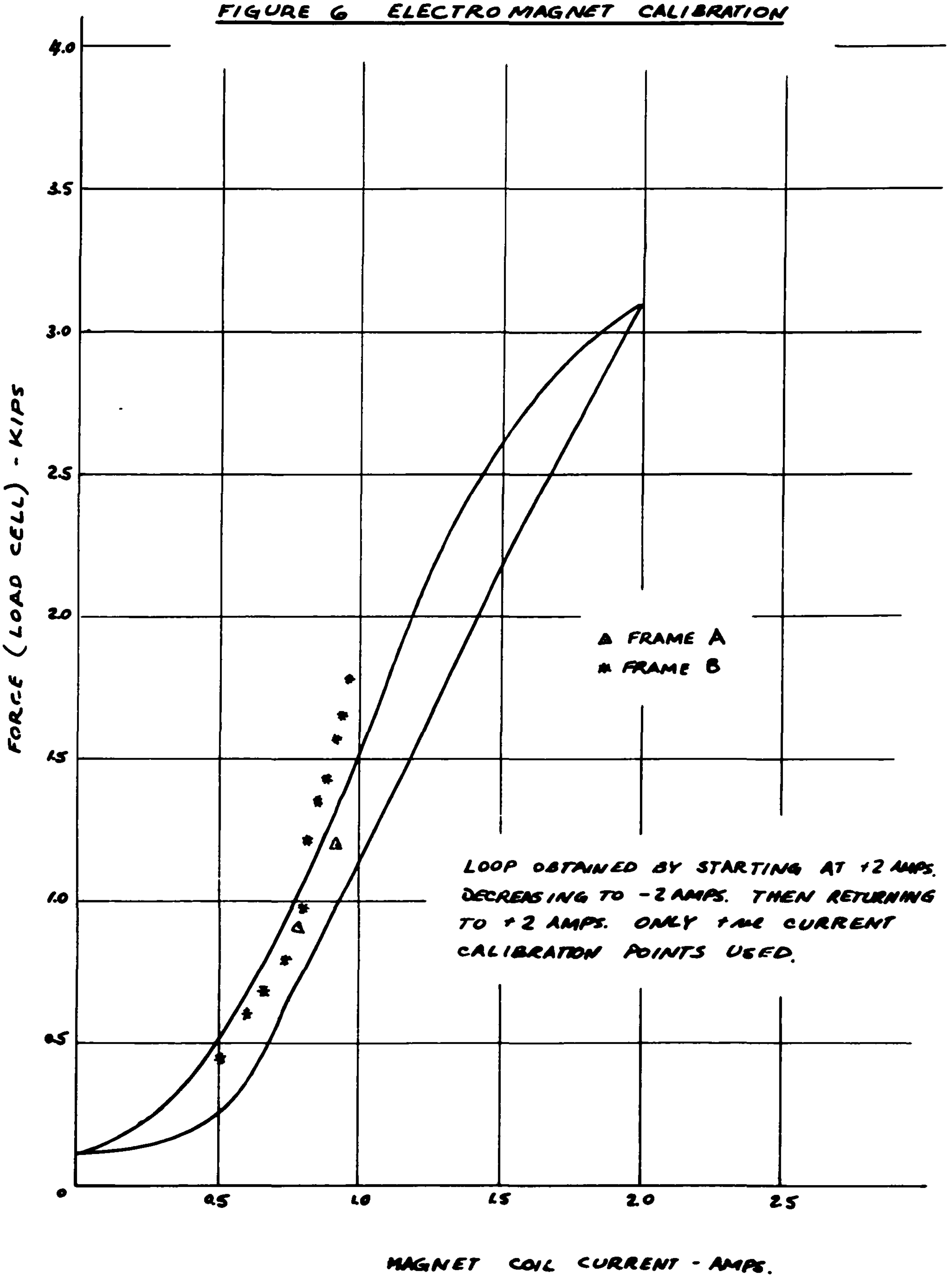

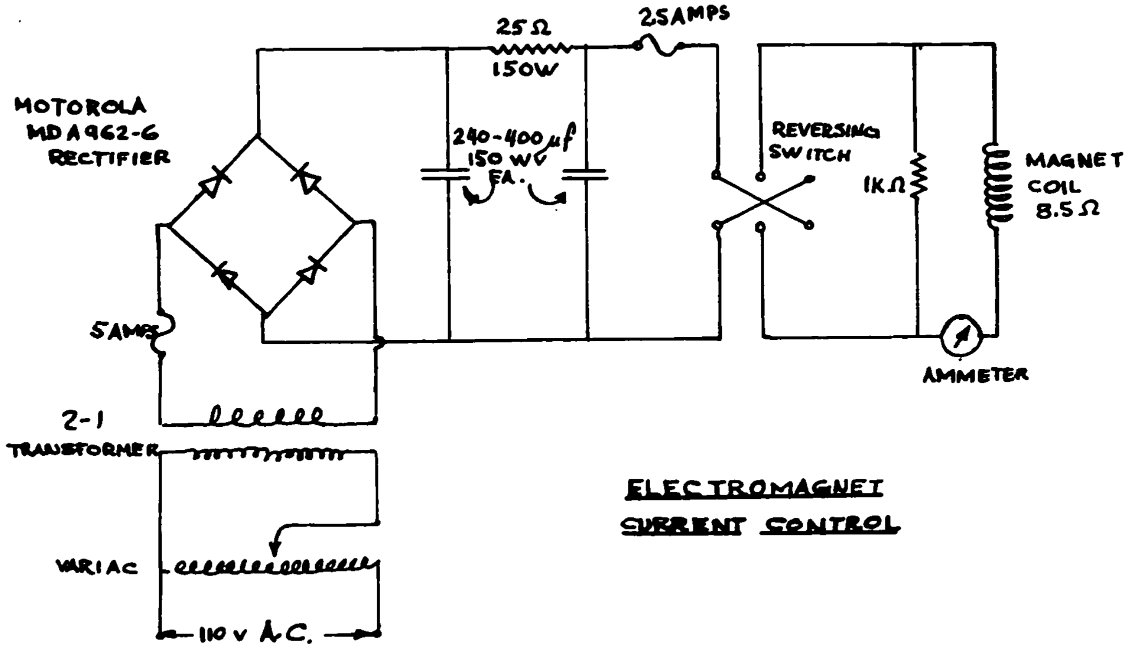

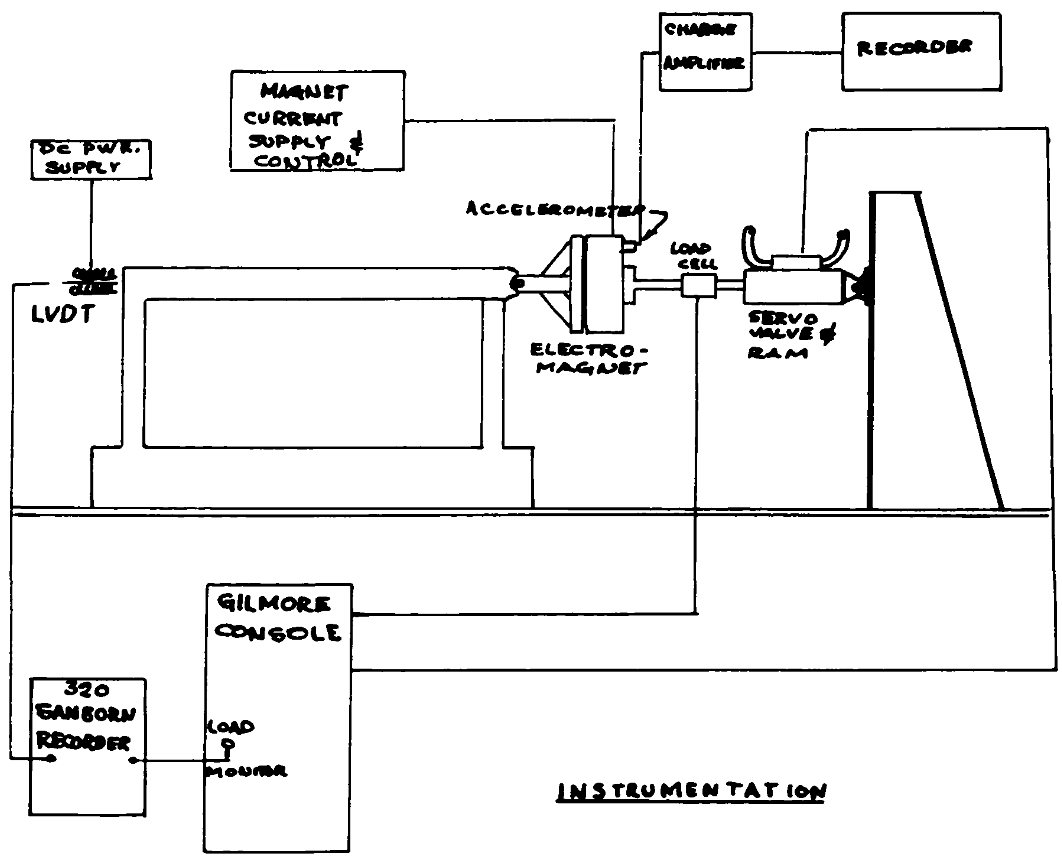

FIGURE 7 INSTRUMENTATION & ELECTROMAGNET CURRENT CONTROL

monitor was calibrated before trials began, checked again before testing Frame A and found not to have varied.

The LVDT was calibrated at a suitable voltage using precise dimension blocks ($\pm$ .0001 inches) before each test.

2.2 Electromagnet

The peak load during an impact was determined by the electromagnet. During the calibration tests the electromagnet gave variable breaking loads at the same current when tested in different setups and on different days. The magnetic flux measured with the search coil appeared to give a better indication of the magnetic force than the current through the magnet coil. Due to magnetic hysteresis and residual magnetism it was found preferable to approach the required current following a particular current path and reverse the current a few times before setting the required value. At the beginning of each test the electromagnet was brought into contact with the pull-off plate, the current was turned up to +2 amperes and reversed about eight times, then starting at +2 amperes the current was decreased to the required value. This same procedure was followed in making the calibration curve, Figure 6. Photo 10 shows the current supply circuitry and Figure 7 a schematic and instrumentation layout.

Figure 6, the electromagnet calibration curve (obtained by impacting against a bulkhead) shows that the results of Frame B do not fall within the calibration loop. This may be due to the different magnetic field influences when the bulkhead (calibration tests) was replaced with the frame specimens as well as atmospheric influences on the air gap material.

An accelerometer was mounted to the back of the electromagnet (see Photo 9) for tests on Frames D and E to assess the magnet's inertial contribution to the load cell force. The output from the accelerometer, a Clevite type 25D21, was amplified in a Kiesler S/N 1129 charge amplifier and recorded on a Hewlett-Packard 7100B strip chart recorder.

Aluminum guides to avoid side-wise motion of the pull-off plate and aluminum chair to provide an air gap and sliding surface between the magnet and its support are shown on Figure 3 and Photos 3, 9 and 11.

2.3 Static Test Apparatus

The apparatus and instrumentation was slightly changed for the static test on Frame C.

The Gilmore pulse generator was disconnected and the servo control input was fed with a variable D.C. potential (3 volts maximum) which allowed a static operation of the Gilmore ram. The static force was measured with a four arm strain gauge loadcell made from a bored aluminum rod (see Photo 6). The loadcell's strain versus load characteristic was found using the structures laboratory Instron testing machine and a BLH SR-4 strain gauge indicator. The lateral deflection of the frame was measured as it was during impact tests and recorded on the Sanborn 320 recorder.

Sixteen strain gauges, Tokyo Sokki Kenkyujo Co. Type PL-20, were mounted on Frame C at locations shown on Table 4.

The gauges were mounted on a surface prepared with an epoxy filler compound using Eastman 910 cement and later waterproofed (see Photo 6). The strains were recorded using the Budd Datran I automatic digital strain indicator with a digital printout unit.

The setup, alignment, weights, etc. for Frame C were the same as for the other frames.

III. MODEL FRAMES AND MATERIALS.

3.1 Similitude

The use of micro-concrete models to study the behaviour of prototype reinforced concrete structures is not fully accepted, to date, due to the necessary inclusion of distortion, size effects and the lack of comparative model prototype studies. Aldridge and Breen [11] have shown excellent agreement between test moments and moments calculated using standard prototype methods for one-eighth scale models of lightly reinforced beams. For another investigation Sabnis and White [8] found a good comparison between 18 model and 2 prototype reinforced concrete frames under monotonic, repeated gravity, and horizontally reversed loading. They found cracking similitude was good even though the prototype tended to deform and crack more at column-beam joints than the model and generally good agreement between model and prototype behaviour.

Leibich [1] gives a dimensional analysis maintaining similitude of elastic and gravity forces and overall mass. Structures where distributed mass would have a greater effect on the modes of vibration would require derivation of scale factors on the basis of appropriate similitude laws. Borges and Pereira [10] discuss how it is impossible to simulate inertial gravity and elastic forces on a structure at the same time and the aspects of behaviour influenced when similitude laws are derived distorting either gravity or elastic force. Reference [1] similitude has a distorted unit mass scale, i.e. the model material is six times too light so that the distributed mass effect is not simulated. This distortion will not have a large effect on this particular model structure due to the relatively stiff beams and the fact that most of the dead load is concentrated at beam level and the structure itself contributes only a small amount to the mass.

The effects of strain rate and damping capacity of model reinforced concrete have yet to be clearly established [12]. From this study damping values vary from 1.5% to 6% of critical damping which compares well with tests done on actual buildings averaging about 5% [7], considering the lack of auxiliary energy absorbing elements on the model. There was strong evidence of strain rate increasing the effective plastic frame resistance. This is discussed in Section 6.3.

Figure 8 gives a forming and reinforcement plan for the model frames taken from reference [1], which also contains further details and a bar list.

3.2 Reinforcement

The reinforcement supplied by Lundy Fence Co. having been cold deformed exhibited no distinct yield plateau as might be found in the hot deformed reinforcing bars used in construction. To obtain a distinct yield plateau the bars were normalized at a commercial heat treater by

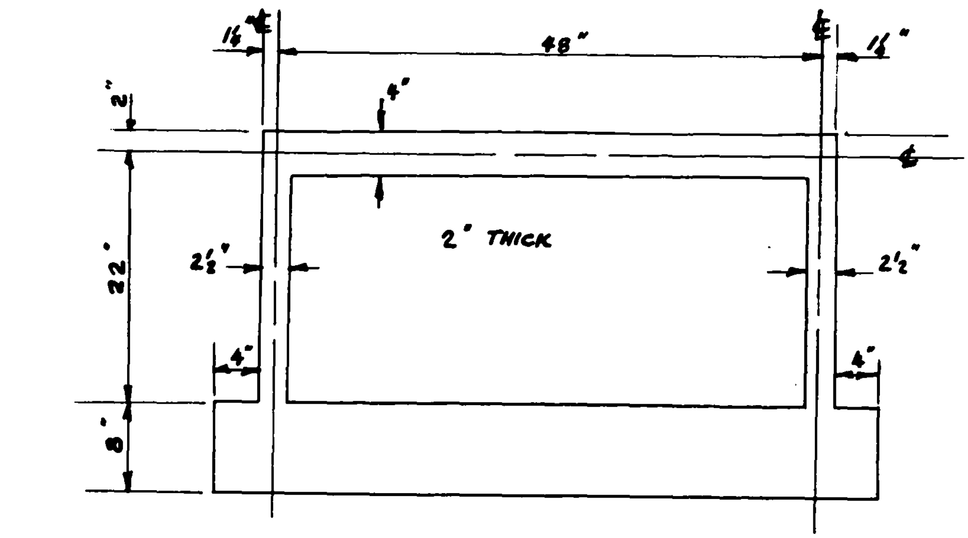

FORMING

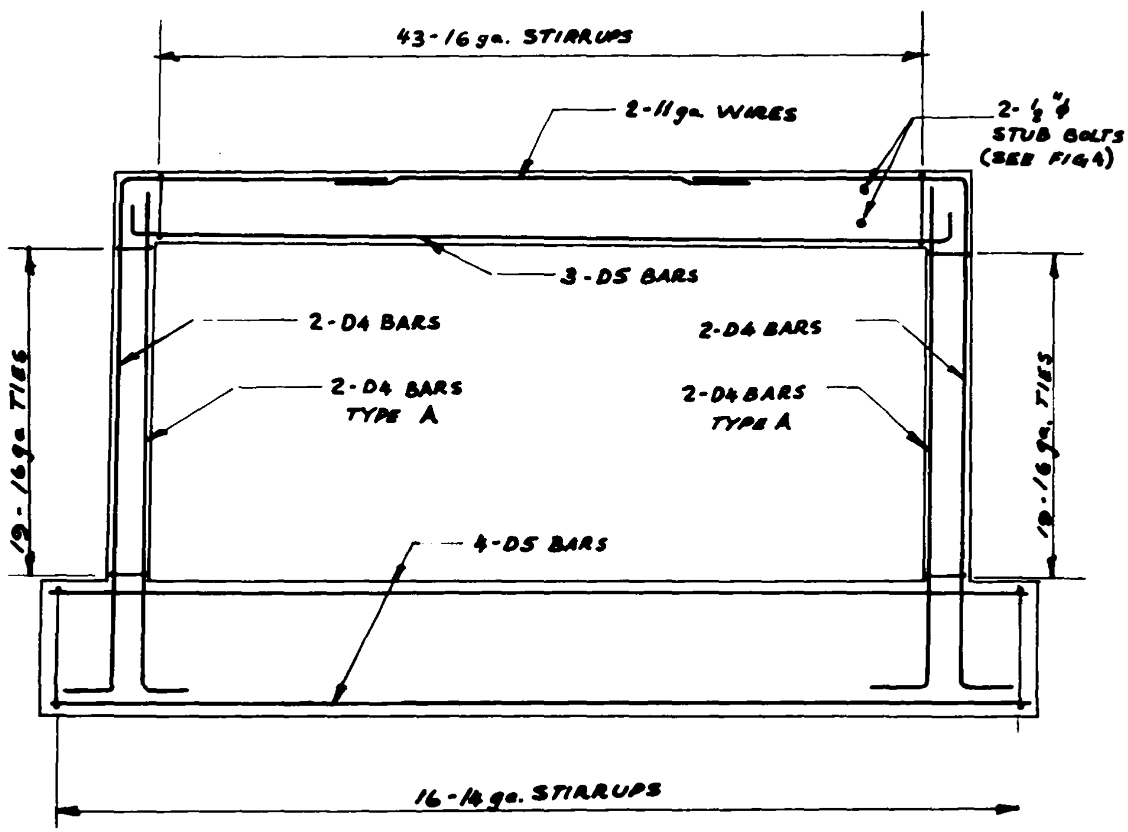

REINFORCING

NOTES
1) AFTER REF. I FOR DETAILS AND SECTIONS SEE REF. I
2) COVER ¼"
3) FRAME THICKNESS 2"

FIG.8 MODEL FRAME

FIGURE 9 STEEL PROPERTIES

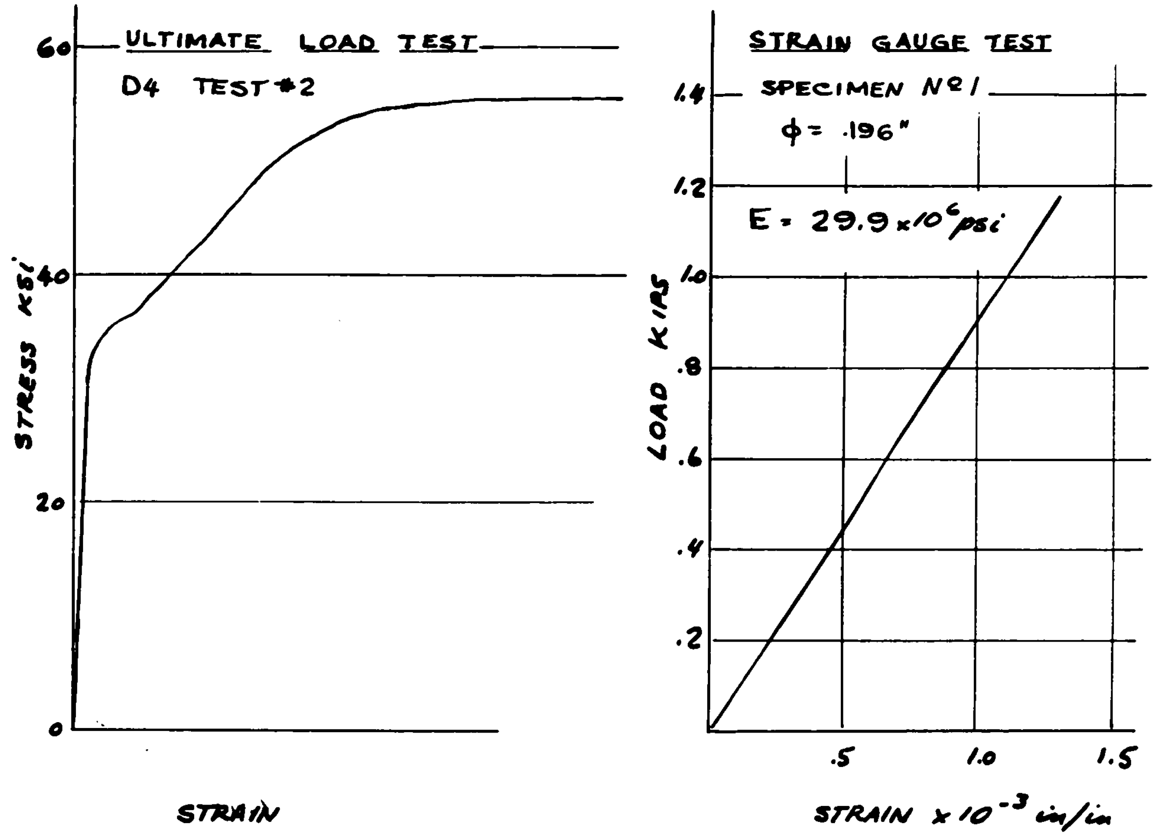

TYPICAL NORMALIZED STEEL TEST CURVES D-4 BAR

AVERAGE YOUNG'S MODULUS FOR D-4 BARS 29.5×10^6 psi

TEST RESULTS FOR NORMALIZED MODEL FRAME REINFORCEMENT

BAR SIZE	Nº OF BARS TESTED	AREA in²	AVERAGE YIELD STRESS KSI	AVERAGE ULTIMATE STRESS KSI	SURFACE	SPEC.
D5	4	.05	35.6	52.5	DEFORMED	ASTM A496-64
D-4	3	.04	36.0	55.8	do	do
11 ga	2	.0114	32.9	50.5	PLAIN	ASTM A82-62T
13 ga	3	.00657	33.4	48.7	do	do
14 ga*	3	.00543	45.3	61.4	DEFORMED	—
16 ga	3	.00307	34.5	50.5	PLAIN	—

* 14 ga. WIRES WERE NOT HEAT TREATED

soaking for one-half hour at 900 degrees Centigrade in a preheated furnace or salt bath then quenching in still air. Figure 9 shows strength results from the reinforcement as it was used. These results show an average yield stress of 36 Kips per square inch for the vertical column steel with an average Young's modulus of 29.5 Kips per square inch.

Yield and ultimate strengths were obtained from specimens of rebar tested in the Instron testing machine, but due to slipping of the grips no precise strain scale could be established. The modulus of elasticity was found from mounting a 10 millimetre long strain gauge on a D-4 size bar from which the deformations had been removed and plotting the stress-strain relation for the linear region using the Instron testing machine and a BLH SR-4 strain indicating box.

3.3 Micro-concrete.

Table 1 lists the average results of tests on control cylinders of each frame as well as curing information and the mix. Reference [23] was used to design the mix.

The model frames were cast on their side. The forms for the frame were made from 2" x 2" x 1/8" angle bolted to a 3/4" sheet of waterproofed plywood. The forms were coated with form oil before each casting. The fresh micro-concrete was consolidated with a form vibrator and trowelled smooth. The fresh concrete was put in the fog room (100% relative humidity) shortly after casting and stripped one

TABLE 1 MICROCONCRETE

FRAME	7 DAY	AT TIME OF TESTING			MIX	
	Average of 6 Cylinder	Average of 3 or 4 cylinders		One Cylinder	AGGREGATE	
	f'_c psi	f'_c psi	f'_t psi	Ec psi x 10^6	MESH SIZE	PERCENT BY WEIGHT
A	4570	6220	608	4.04	10	20
B	4480	6440	612	4.11	16	20
C	4050	6950	602	3.12	24	25
D	4560	7450	670	3.68	40	25
E	4910	7450	683	4.37	70	10
Average	4514	6902	635	3.86	WATER CEMENT RATIO = .6 AGGREGATE CEMENT RATIO = 3.25 BOTH BY WEIGHT	

NOTES:

1) Cylinders were all 3" x 6".
2) Unit weight of specimen frames was 145 pounds per cubic foot.
3) Cylinders for f'_c and Ec tests were capped with plaster of paris.
4) 7 day cylinders were cured in fog room at 100% relative humidity until a day before testing. Other cylinders and specimen frames had from two to three months curing in fog room and were dried in the laboratory for at least one week before testing.
5) The microconcrete was made in 1.25 cubic foot batches in a 3 cubic foot capacity Eirich rotating paddle mixer.
6) The aggregate was crushed quartz supplied by Industrial Minerals of St. Jerome, Quebec. Mesh sizes refer to their standards.
7) High early strength Portland cement supplied by Canada Cement Company was used.

or two days later.

Figure 10 shows the stress-strain curve for Frame C concrete which was obtained using a BLH SR-4 strain indicating box and two 20 millimetres long strain gauges mounted on the surface of a 3" x 6" cylinder on diagonally opposite sides. The concrete was treated with an epoxy filler compound in the region of the gauges before they were applied.

FIGURE 10 FRAME C STRESS - STRAIN CURVE FOR CONCRETE

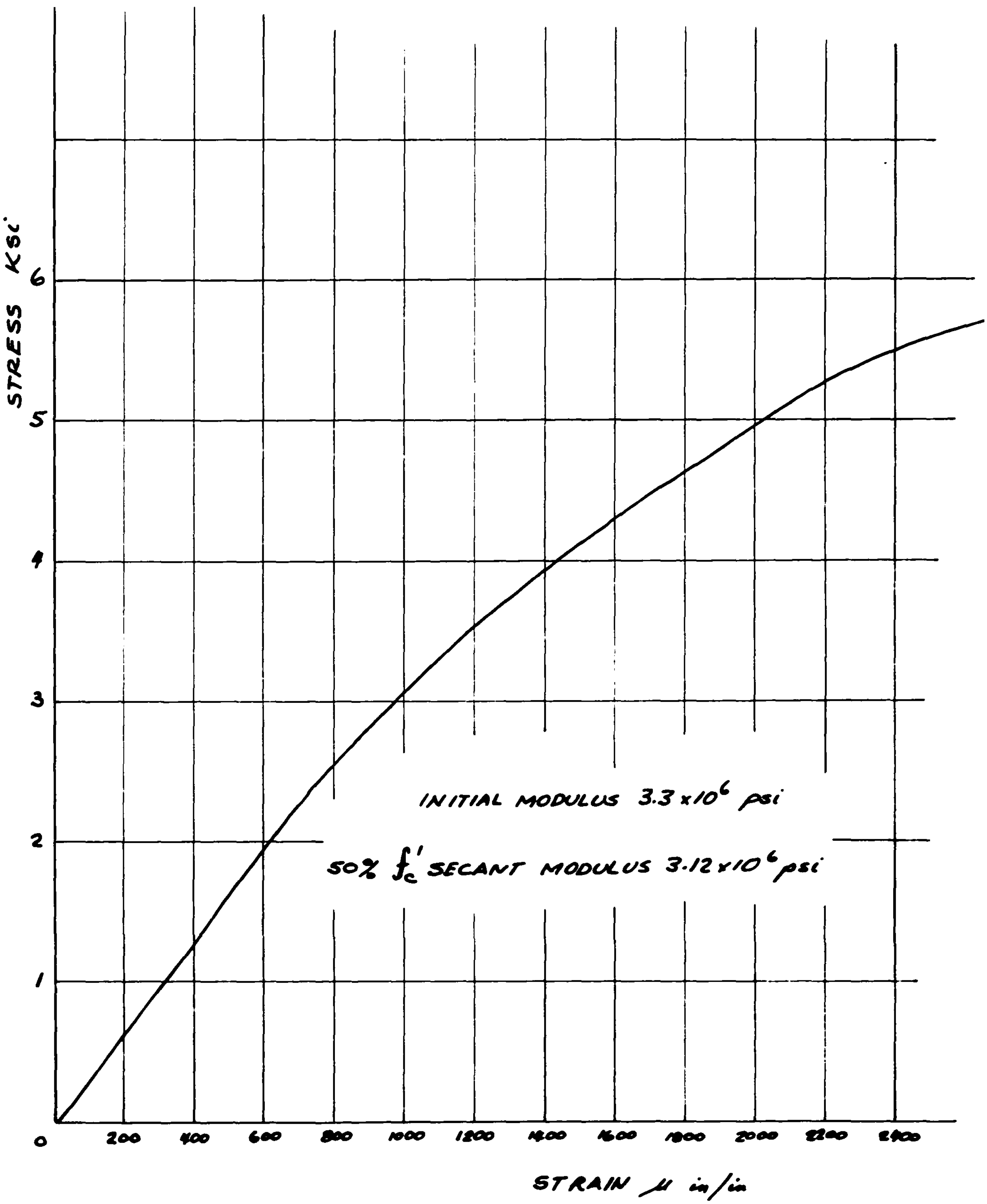

IV. PROCEDURE & OBSERVATIONS

4.1 General

The laboratory investigation involved testing four Frames A, B, D and E with lateral impact loads and Frame C with lateral static load.

Frame A was loaded with 20 impacts of approximately 900 pounds peak force, followed by 10 impacts of approximately 1200 pounds peak force. The final Test A-31, was an attempt to give the frame a triangular impact with 1500 pounds peak force.

Frame B was loaded with 14 impacts, each successive impact designed to have a peak force 100 pounds greater than the previous.

There was only one test run on Frame D which attempted to subject the frame to the same impact that was given to Frame B Test 12, the main difference being that the frame had a previous history of yielding in the reversed direction, i.e. reversed plasticity.

The Frame E series of tests was similar to that of Frame B. It was attempted to increase the initial rate of loading and an accelerometer was attached to the electromagnet to determine its inertial force during impact.

Frame C static testing involved three loading phases and two unloading phases of repeated lateral force. The frame was loaded to ultimate resistance on each loading phase. Strain readings were obtained for the first loading phase at the hinge locations on the frame columns.

In order to check for relative movement between the frame and the mass at the weight clamps shellac was painted around the bearing blocks for the Frame B series of tests. During testing these areas were checked for relative movement; none was apparent even after the last test. The frame base beam showed no visible sign of distress where it bore against the end brackets beyond that caused by setting up and alignment procedures. When the side plates (Figure 4) were removed from the stub bolts which transferred the impulse to the frame there was no noticeable crushing of concrete around the bolts.

From the deflection response records simple calculations were made and used for graphs and program input (Tables 2, 3 and 5). Frequency and damping calculations could generally be made only over six or seven cycles of the free response. The first peak in the free response was always taken as the first positive, deflection in the direction of the lateral force, peak after the linearized decay period of the impulse had returned to zero. For some tests the force response records appeared irregular in amplitude and period and it was difficult to accurately evaluate the frequency and damping.

4.2 Frame A.

Table 2 contains observations and calculations from the recorded deflection response and impacts for Frame A tests. This series of tests was designed to repeat the same impact

TABLE 2 FRAME A RESULTS

TEST	Y MAX. in.	Y RES. in.	ACCUM Y RES in.	n	A_1 in. x 10^{-3}	δ *	f Hz	TR sec.	TI sec.	FI Kips	K ** K/in.
1	.089	.010	.010	2	2.5		12.5	.09	.20	.88	10.64
2	.091	.003	.013	4	2.5		11.43	.085	.195	.92	8.93
3	.096	.004	.017	4	3.8		12.5	.095	.19	.94	10.64
4	.094	.001	.018	6	5.1		10.90	.09	.20	.87	8.11
5	.112	.002	.020	6	5.1		11.54	.085	.19	.93	9.1
6	.104	.002	.022	6	5.1		11.54	.09	.19	.92	9.1
7	.106	.003	.025	6	5.1		11.65	.08	.185	.90	9.26
8	.102	.002	.027	6	6.4		11.10	.1	.19	.86	8.40
9	.106	.002	.029	6	6.4		11.10	.1	.19	.90	8.4
10	.107	.001	.030	6	6.5		11.10	.09	.18	.90	8.4
11	-	.002	.032	6	8.3	.14	11.67	.09	.185	.95	9.26
12	-	.002	.034	6	8.3	.15	11.65	.1	.19	.94	9.26
13	-	.003	.037	6	6.7	.15	11.76	.09	.185	.98	9.42
14	-	.001	.038	6	7.9	.19	11.10	.09	.19	.92	8.40
15	-	.002	.040	6	8.0	.15	11.53	.095	.18	.92	9.10
16	-	.002	.042	6	8.0	.15	11.56	.09	.185	.93	9.12
17	-	.002	.044	6	8.3	.17	11.44	.09	.18	.92	8.94
18	-	.002	.046	6	8.4	.16	11.65	.09	.185	.94	9.26
19	-	.002	.048	6	8.9	.17	11.64	.095	.185	.92	9.26
20	-	.001	.049	6	8.7	.17	11.52	.09	.18	.87	9.07
AVE						.16	11.52			.914	
21	-	.012	.061	7	11.1	.20	11.3	.09		1.21	8.72
22	-	.009	.070	7	9.2	.19	11.48	.09		1.18	9.00
23	.142	.009	.079	7	12.2	.26	11.1	.09		1.20	8.40
24	-	.006	.085	7	12.0	.22	11.0	.09		1.19	8.26
25	-	.005	.090	7	13.8	.21	10.93	.10		1.17	8.16
26	-	.008	.098	7	14.3	.20	10.93	.09		1.21	8.16
27	-	.007	.105	7	15.0	.20	10.93	.09		1.23	8.16
28	-	.006	.111	7	15.2	.20	10.93	.10		1.22	8.16
29	-	.010	.121	7	15.6	.21	10.93	.10		1.22	8.16
30	-	.014	.135	7	15.0	.20	10.93	.10		1.22	8.16
AVE	-					.20	11.04	.10		1.21	
31										1.54	

* $\delta = \frac{1}{n} \ln \frac{A1}{An}$ ** $K = (2\pi f)^2 M$

at 900 pounds peak force (tests 1 to 20) then increase the peak force to 1200 pounds for another ten impacts (tests 11 to 21). Test A-31, Figure 18, was an attempt at giving a triangular pulse of 1500 pounds peak force and constituted a failure pulse. For the first ten tests the LVDT output was scaled so that the total response including maximum deflection was recorded. For all the other tests, except A-23, this scale was increased so that a more substantial record of the free response was obtained. Due to this increase in scale the peak and higher portions of the forced response were off the record. Figure 11 shows the Test A-12 record.

The residual plastic sidesway deflection after Test A-31 was 1-1/8 inches.

4.3 Frame B.

The tests on Frame B were designed to apply successively greater impacts to the frame until failure. The free response was recorded on a large scale for all except Test 12 from which the total response was obtained (see Figure 12). Observations and calculations are given in Table 3.

The early tests had much lower initial rates of loading than the later tests, the maximum difference being about three times. Nonetheless, the peak load could be reasonably well controlled.

Total permanent sidesway after Test 14 was 15/16 inches. Figure 18 shows the impact for Test B-14.

TABLE 3 FRAME B RESULTS

TEST	Y MAX in.	Y RES in.	ACCUM Y RES in.	n	δ *	f Hz	TR sec.	TI sec.	FI Kips	K ** K/in
1	.035	.004	.004	7	.10	13.33	.065	.18	.42	12.13
2		.003	.007	7	.09	12.92	.065	.19	.575	11.37
3		.002	.009	7	.14	12.65	.070	.195	.650	10.92
4		.004	.013	7	.15	12.83	.08	.19	.775	11.36
5		.004	.017	7	.17	12.34	.08	.19	.950	10.41
6		.001	.018	7	.18	12.18	.09	.195	1.21	10.30
7		.001	.019	7	.15	12.1	.08	.19	1.21	10.00
8		.005	.024	-	-	12.6	.09	.20	1.34	***
9		.008	.032	-	-	-	.095	.205	1.42	***
10		.027	.059	5	.22	12.05	.09	.20	1.59	9.930
11		.081	.140	7	.24	11.38	.095	.23	1.65	8.84
12	.218	.066	.206	7	.31	10.07	.10	.24	1.62	9.91
13		.246	.452	4	-	9.76	.095	.30	1.72	-
14		.244	.696	5	-	9.04	-	-	1.74	-

* See Table 2

** See Table 2

*** Records difficult to evaluate. Test B-8 coincided with noticing of cracks in Joints 1 and 3. After B-10 cracks noticed in all joints.

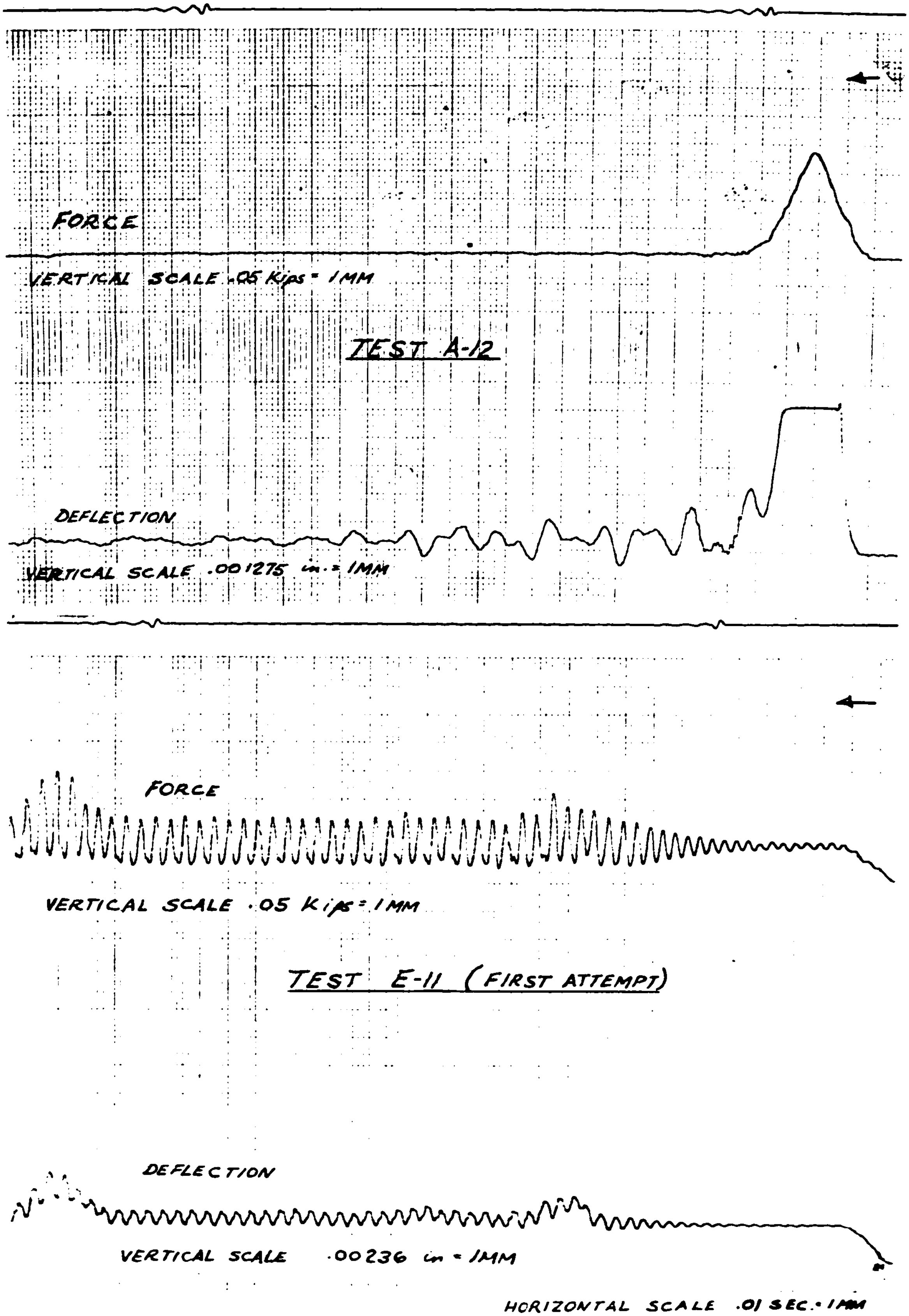

FIGURE 11 TESTS A-12 & E-11 RECORDS

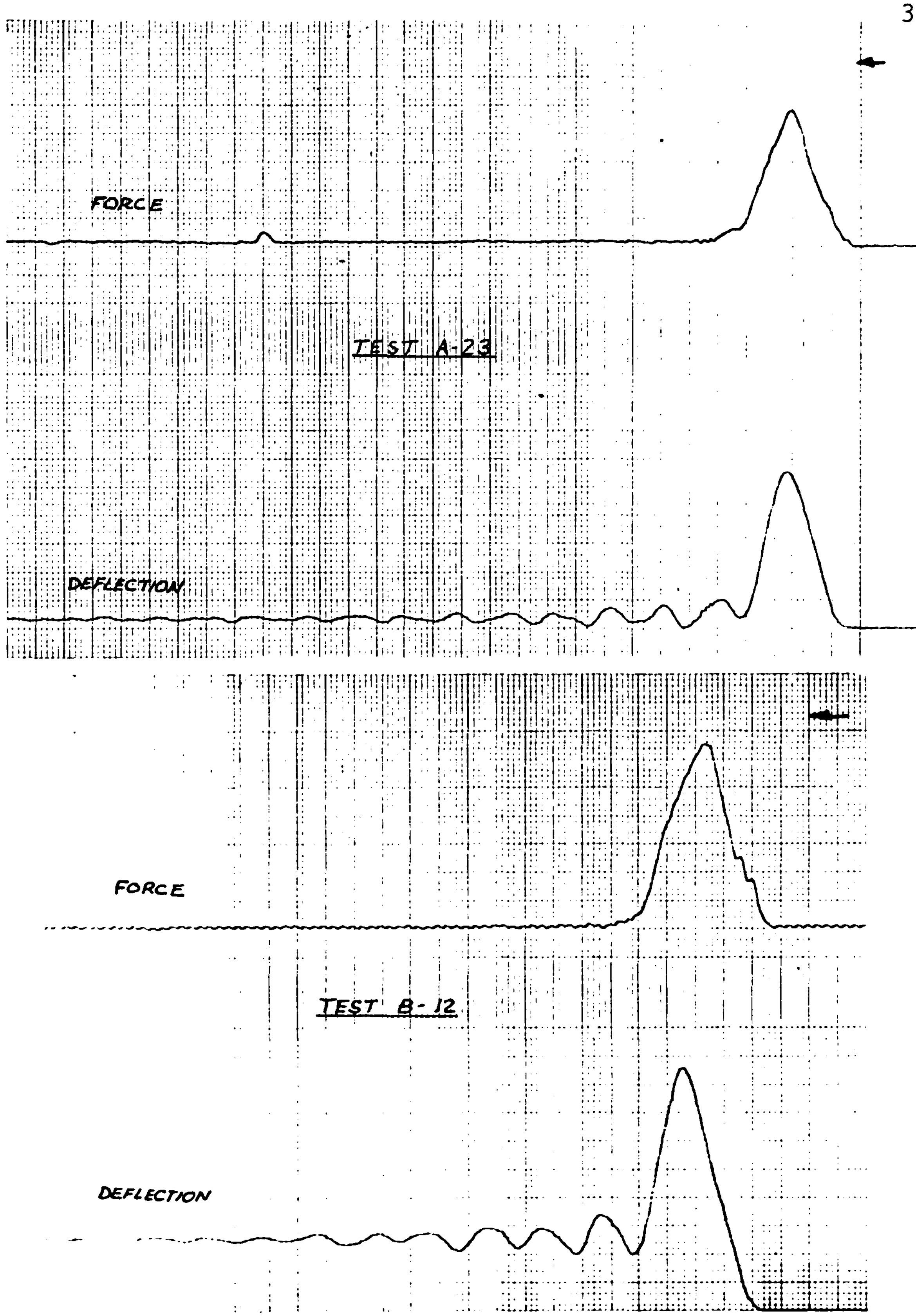

SCALES VERTICAL .05 Kips = 1 MM HORIZONTAL .01 SEC. = 1 MM

FIGURE 12 TESTS A-23 & B-12 RECORDS

4.4 Frame C Static Test

Three loading phases and two unloading phases were applied to Frame C. Lateral deflections and strain gauge readings were made at 100 pound increments.

Four strain gauges were mounted at each hinge location on the columns as shown in Table 4 and Photo 5. Strains were obtained for the first loading phase and averaged values are given in Table 4 and plotted on Figure 13. After the ultimate resistance was reached on the first loading phase most of the strain gauges had stopped giving meaningful readings.

When the frame reached its ultimate resistance on first loading the deflection increased to about 1.45 inches before the load was decreased enough to stabilize the movement. The plotted points of the first loading phase of Figure 14 indicate at least two abrupt increases in deflection; one at 200 pounds and another at 600 pounds, as well Figure 13 indicates an abrupt strain increase at 600 pounds lateral load. This effect is probably caused by bond slip and cracking at the joints. Subsequent reloading did not show these stages and exhibited a more linear characteristic up to yield than did the first loading points.

The frame stiffness was measured as the slope of the lateral load versus deflection curve, Figure 14, from 0 to 1100 pounds. The values for the three loading phases are 10.4, 8.2 and 8.1 Kips per inch. This deterioration of the stiffness might be partially accounted for with bond slip, deterioration of the concrete matrix and geometric stiffness reduction from the permanent sidesway deformation.

TABLE 4 FRAME C STRAINS

JOINT		ZEROS, NO LOAD	AVERAGE OF 2 GAUGES CORRECTED FOR ZERO, INCHES PER INCH												
			ONLY DEAD LOAD	F= 100 lbs.	200	300	400	500	600	700	800	900	1000	1100 Creeping	1200 Creeping
1	C	+003	-129	-170	-218	-326	-391	-469	-525	-688	-754	-827	-905	-994	-3633
	T	+002	+078	+104	+142	-	-	-	-	-	-	-	-	-	-
2	C	-001	+077	+050	+013	-019	-056	-105	-149	-251	-304	-367	-428	-519	-1043
	T	000	-116	-075	-030	+006	+044	+087	+114	+145	+167	+188	-	-	-
3	C	+002	-043	-071	-119	-195	-241	-323	-435	-595	-671	-758	-857	-1004	-3336*
	T	+009	+055	+095	+139	+196	+243	+301	+338	-	-	-	-	-	-
4	C	+007	-037	-007	-065	-132	-182	-256	-303	-404	-458	-515	-582	-681	-3113
	T	+006	-042	-008	+024	-	-	-	-	-	-	-	-	-	-

NOTES:

1) * Value for only one gauge.
2) C = Compression strain, T = Tensile strain.
3) Typical strain gauge locations, 4 at each joint.

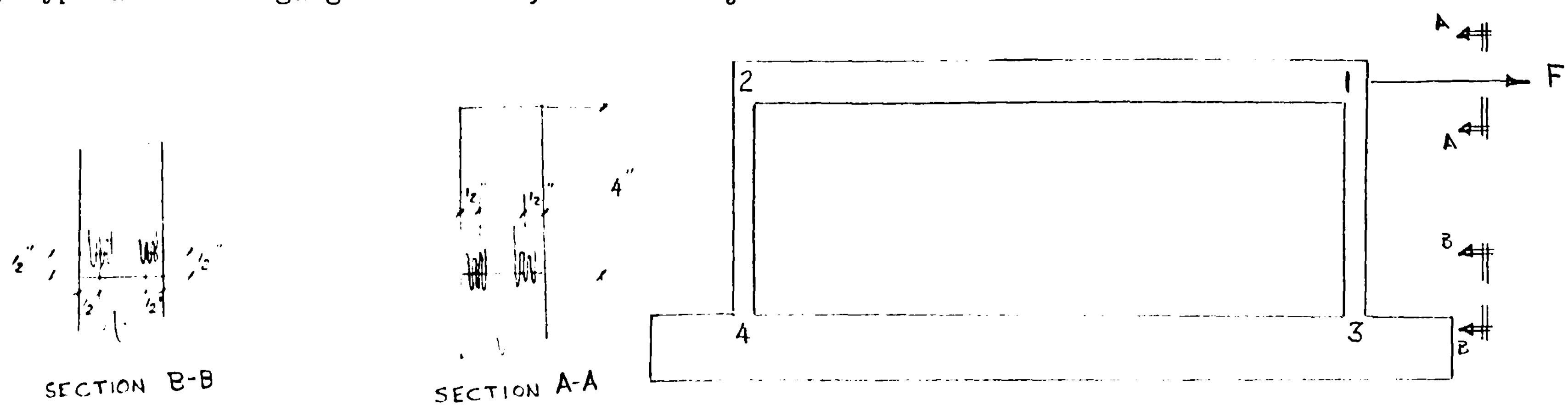

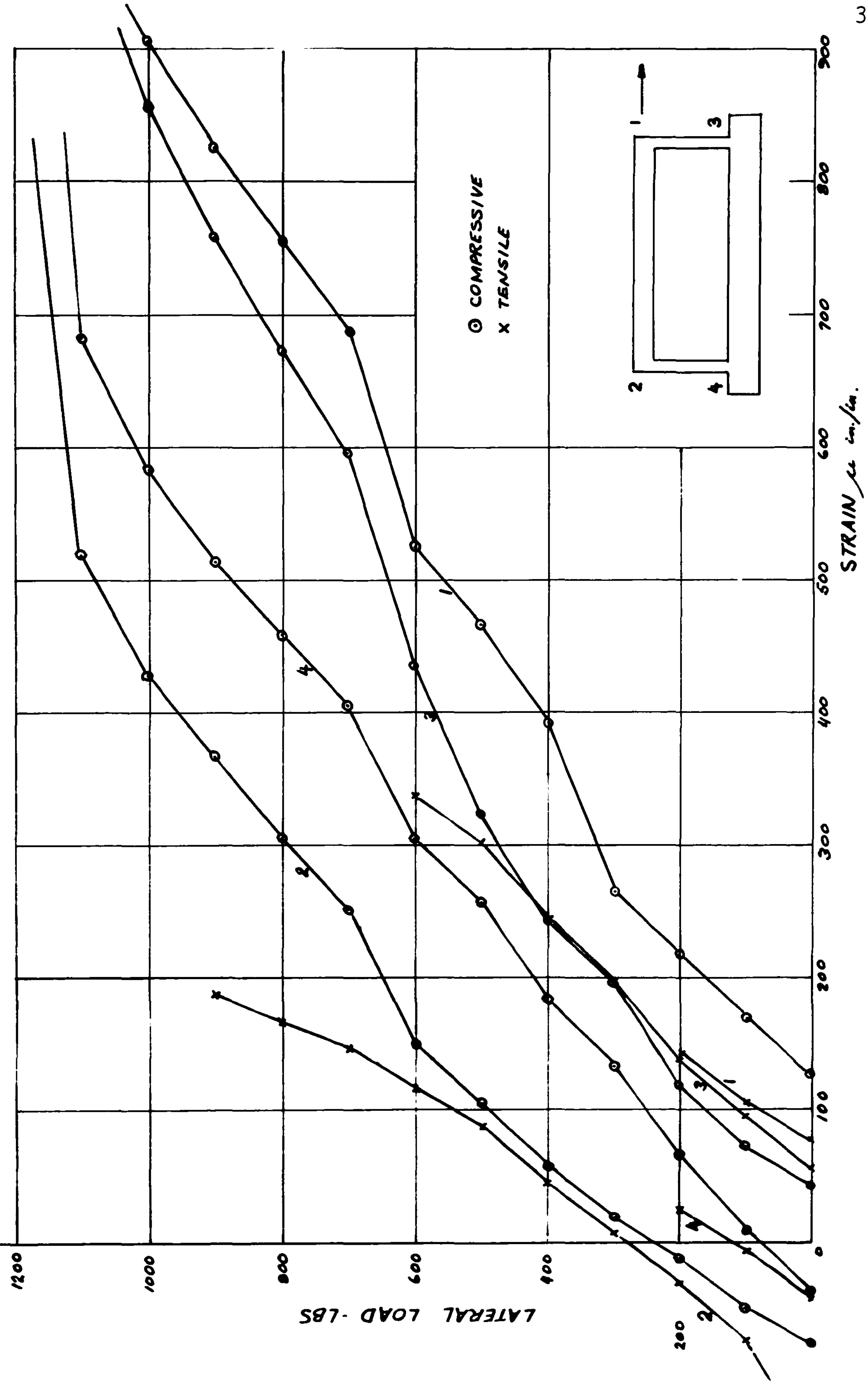

FIGURE 13 FRAME C JOINT STRAINS vs LATERAL LOAD

FIGURE 14 FRAME C LOAD vs DEFLECTION

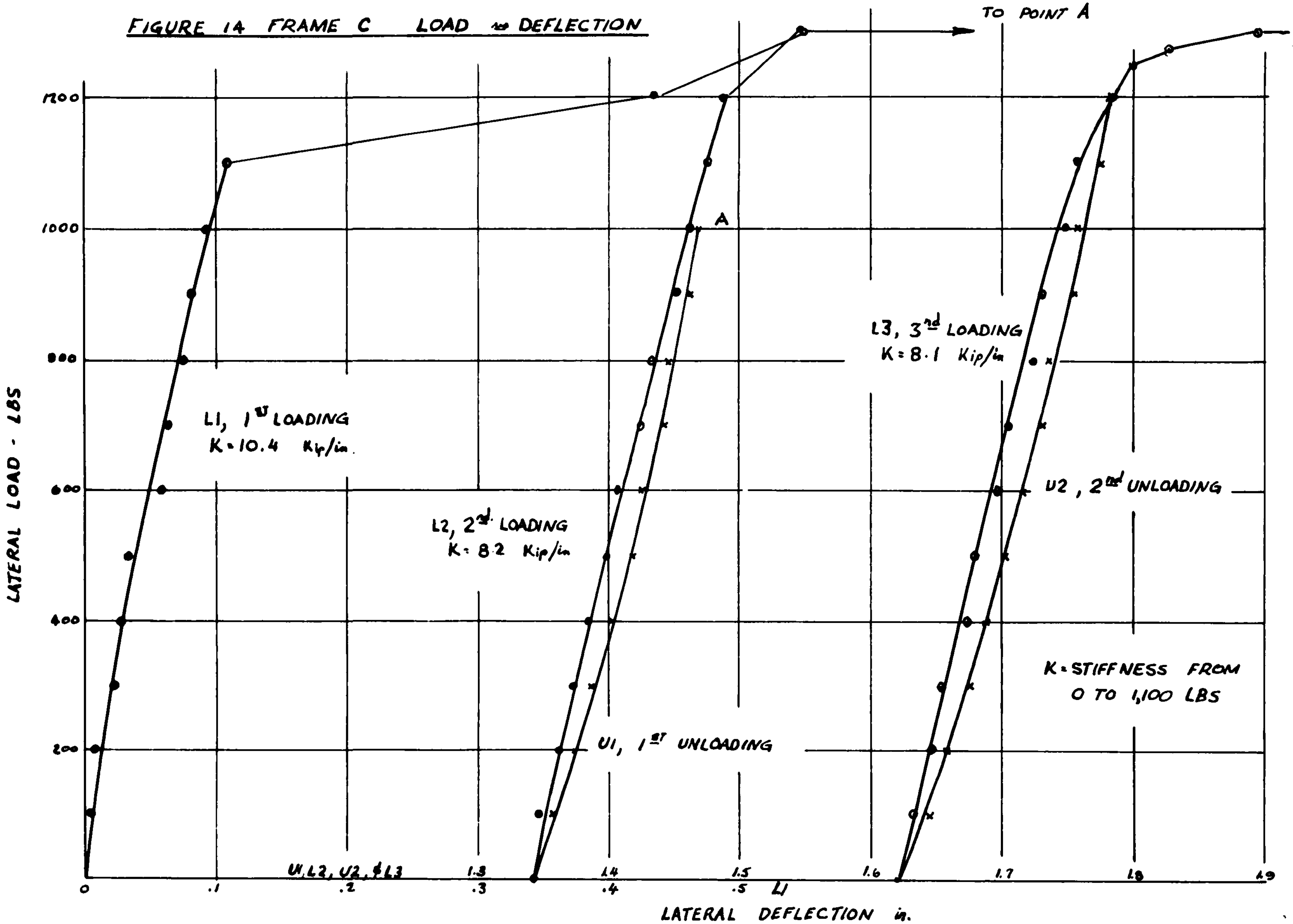

The first loading phase started to yield at a lateral load of 1100 pounds, then increased to an ultimate load of 1300 pounds at .555 inches deflection. Subsequent loading curves showed a higher yield load and a stiffer characteristic between yield and ultimate but the same ultimate load as the first loading.

There was noticeable deflection creep during the static loading tests for loads above 1100 pounds in the first loading phase and 1200 pounds in the second and third loadings. This creep was roughly measured on the third loading phase and indicated .03 inches per second at 1250 pounds then at 1300 pounds an initial creep rate of .8 inches per second which increased rapidly to failure.

A negative stiffness in the frames could not be measured, if it existed, using this loading technique.

The stiffening spring characteristics exhibited by the tensile gauges in Figure 14 is indicative of cracking on the tensile face of the column and the resulting strain relief between cracks. The very high tensile strains recorded in hinges 2 and 3 are likely due to the epoxy filler compound used as a base to mount the strain gauges.

4.5 Frame D.

During the set up of Frame D it was inadvertently loaded beyond yield in the reverse direction (ram in compression rather than tension). The rate of loading was slow and the permanent lateral deflection after retracting the ram was 3/4 inches from the vertical. The dead weight was clamped in place and the frame was aligned before the reversed loading occured.

It was decided to repeat Test 12 impulse of Frame B and see how the frame reacted with an immediate past history of reversed plasticity. Figure 18 shows the impact, the peak load reached was 1.55 Kips and the permanent sidesway deflection was +9/16 inches giving a total plastic deformation of 1-5/16 inches during the test. Unfortunately, the displacement range of the LVDT was exceeded and no record of the free displacement response was obtained.

It is interesting to compare the shapes of final impulses on Frames A, B, D and E, Figure 18. These flat topped shapes are a result of the Gilmore force pulse system not reacting fast enough to give a triangular pulse and are determined, to a large extent, by the load deflection characteristics of the frame. From Figure 18 the maximum force during the impacts occurs near the beginning for Frames A, B and E and near the end for Frame D. This impulse shape on Frame D, which was intended to have an impulse of Test B-12 type, is attributed to the decrease in effective stiffness suffered by reversed plasticity.

4.6 Frame E.

The series of tests performed on Frame E was an attempt at repeating the Frame B series with an increased initial rate of loading, i.e. the Gilmore pulse generator was adjusted so that the slope of the voltage ramp for the first three stages reached its peak in .15 seconds as opposed to .31 seconds for Frames A, B and D. This had a very small effect on the initial load rates.

From the accelerometer readings the maximum inertial force of the electromagnet was in the order of 3.5 pounds which was not large enough to be discerned on the records at the scales used during the tests.

The first attempt at Test 11 resulted in a five second long 40 Hertz oscillating forcing function which reached a peak force of about 1 Kip and was stopped by closing the hydraulic fluid supply valve. The initial part of this record is shown in Figure 11.

This abortive test undoubtedly had some effect on the impulses of subsequent tests and probably resulted from not disconnecting the battery device used to move the Gilmore ram back and forth during alignment.

Table 5 contains results of observations on Frame E tests and Photos 12 to 16 show the frame and joints after the final test.

4.7 Ductility and Hinge Formation

The failure mechanism for all the frames was sidesway as shown in Photo 12 and typical joints after the final tests are shown in Photos 13 to 16.

Column hinges at Joints 1, 4 and 3 formed in a flexural mode; first flexural cracks form and as the load is increased and the neutral axis moves toward the compressive face the concrete crushes. Joint 2 hinge developed in a different manner. Initially cracks on the tension face extended to the location of reinforcement in the compressive zone then the cracking propagated along the compression steel in the pattern shown on Photo 13. The distinct concrete crushing

TABLE 5 FRAME E RESULTS

TEST	Y MAX in.	Y RES in.	ACCUM Y RES in.	n	δ *	f Hz	TR sec.	TI sec.	FI Kips	K ** K/in.
1	.0386	0	0	7	.136	12.65	.057	.195	.424	10.9
2	.0453	.001	.001	7	.157	12.46	.050	.198	.480	10.6
3		.003	.004	7	.177	12.5	.06	.195	.612	10.66
4		.006	.010	7	.215	12.35	.07	.19	.766	10.4
5		.003	.013	7	.238	12.28	.08	.198	.830	11.3
6		.001	.014	7	.280	11.96	.08	.197	.910	9.76
7		.002	.016	7	.278	11.80	.085	.20	1.00	9.5
8		.0359	.052	7	.367	11.47	.085	.21	1.115	8.97
9		.0571	.109	7	.295	11.47	.095	.20	1.175	8.97
10		–		–	–	–	.10	.23	1.35	–
11***		.161		7	.237	10.69	.11	.295	1.37	7.77
12	.43	.245						.29	1.405	
13									1.46	

* See notes on Table 2

** See notes on Table 2

*** First attempt at Test E-11 resulted in oscillating pulse of Figure 11.

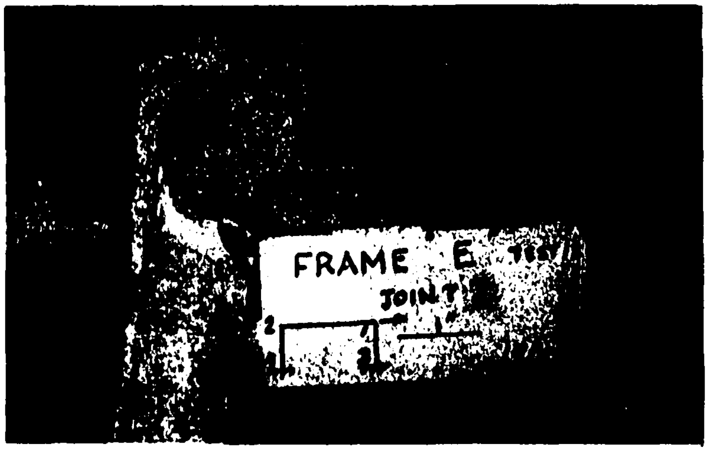

PHOTO 13.

PHOTO 14.

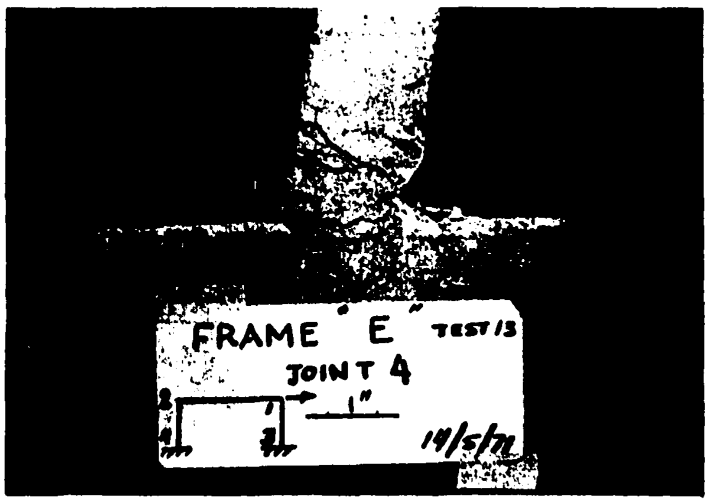

PHOTO 15.

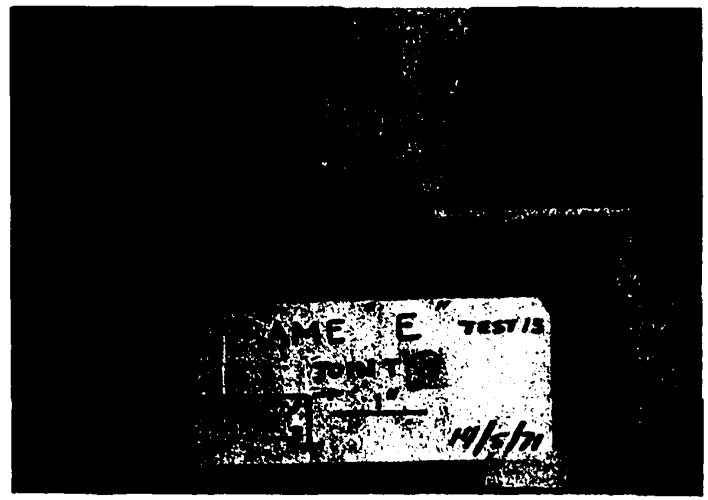

PHOTO 16.

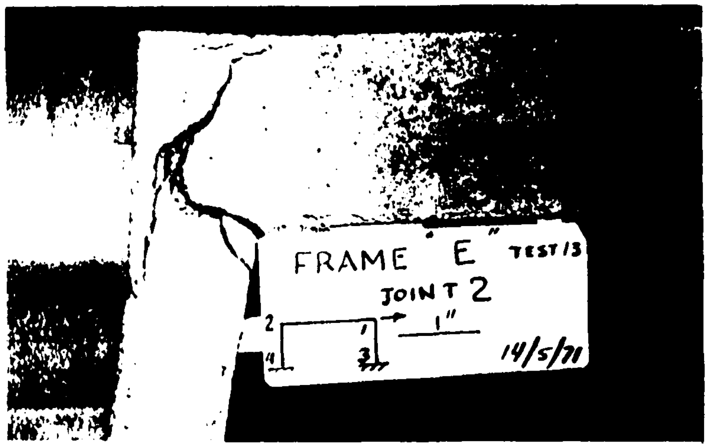

PHOTO 13.

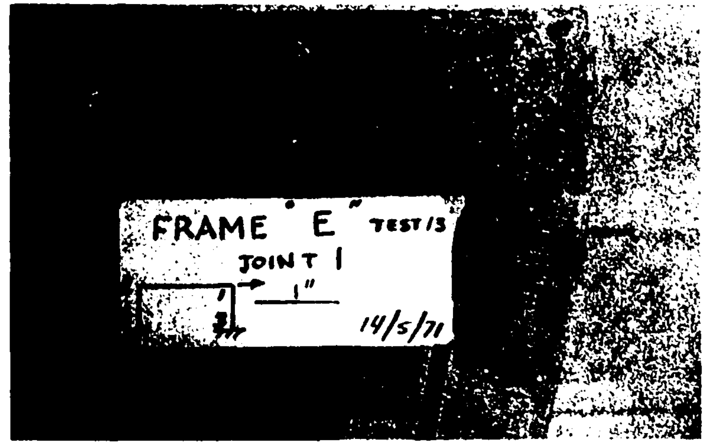

PHOTO 14.

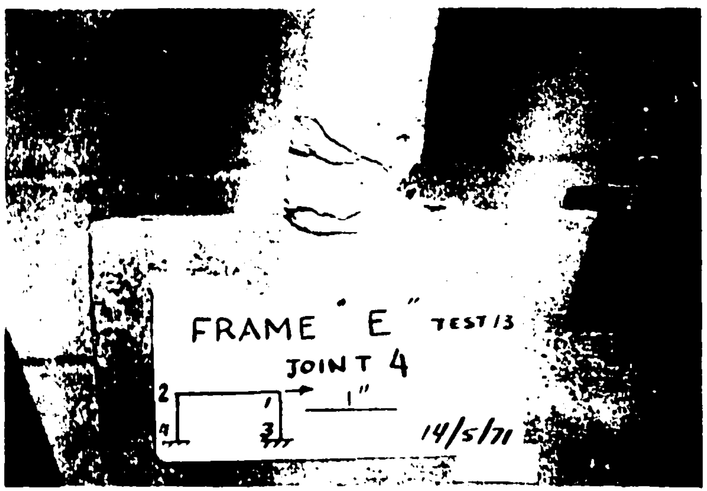

PHOTO 15.

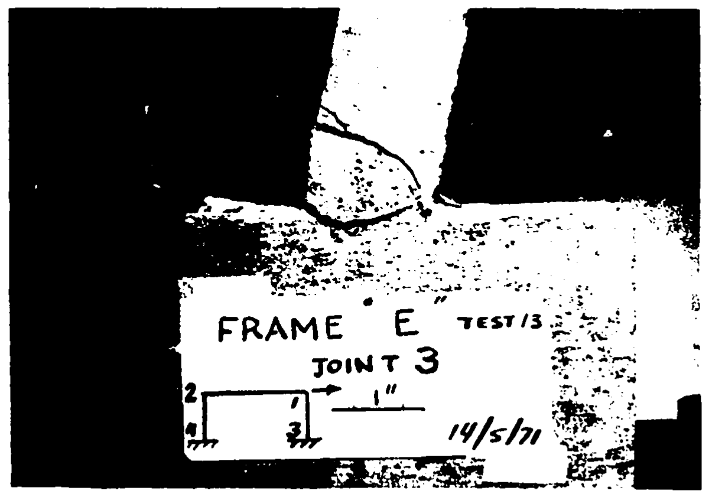

PHOTO 16.

zone is not evident in this hinge and was probably affected by the pulling out of reinforcing bars Type A, Figure 8 which was apparent on close examination of the failed joint. This shear joint type failure is more brittle and would absorb less energy than the hinges at joints 1, 4 and 3.

Ductility in joint 2 might have been achieved by hooking bars type A into the beam and confining the concrete in the joint as recommended by Blume et al [2]. Bate [9] notes that reinforced concrete beams which had failed in a flexural mode under static tests failed in a shear mode under impact with less energy absorption so he concluded that, "under impact conditions, transverse reinforcement fulfills an important role in developing the maximum resistance of a reinforced concrete beam which cannot be assessed from the results of static tests."

Test E-12 showed a ductility factor of 3.9 (maximum displacement/static first loading yield displacement of Frame C) and represented the maximum observed as most of the peak deflections exceeded the recorder scale range. The first loading phase of Frame C static test realized a ductility factor of approximately 13 which greatly exceeds recommended values of 4 to 6 given by Blume et al [2].

V. CALCULATIONS

5.1 Elasto-Plastic Response Analysis

After observing the static force deflection curve for first loading of Frame C, Figure 14, it was decided to analyse the frames assuming a simplified elasto-plastic force deflection characteristic. The first loading phase of Figure 14 might be considered for discussion as a linear portion up to 1100 pounds and a reduced stiffness curve to 1300 pounds. On the first loading curve of Figure 14, 1300 pounds was reached at a deflection of .555 inches representing a deflection to height ratio of 1/40. Blume [1] has noted that the assumption of elasto-plastic behaviour beyond the yield point is conservative with respect to the actual bilinear characteristic but liberal with respect to the deterioration and loss of initial stiffness under reversals and cycling. He also notes that these effects tend to cancel each other out as far as energy capacity is concerned. The second and third slopes of load deflection curves, Figure 14, show the deterioration in stiffness from the first loading phase.

For the mathematical model a single degree of freedom, elastic perfectly plastic, viscously damped system was assumed. The effects of distributed mass and the predominance of the sidesway mode of response are discussed in Section 3.1. The elasto-plastic idealization is general practice for solving structural dynamics problems; as is, expressing damping in reinforced concrete by an equivalent viscous coefficient [2] for damping less than 10% of critical. The equivalent viscous coefficient was calculated from the logarithmic decrement of the free deflection response.

$$\delta = \frac{1}{n} \ln \frac{A_1}{A_n}$$

Ratio of critical damping = $\delta / 2\pi$

The frame stiffness during the dynamic tests was approximated from the observed response frequency on the basis of a single degree of freedom, linear undamped oscillator; where stiffness = $(2\pi f)^2 M$. For damping less than 10% critical this is a good theoretical estimate.

The response program input included a linearization of the triangular impact and as discussed in Section 6.4 is probably an overestimate for the decaying portion. The yield frame resistance was taken as 1100 pounds, that observed from the first loading phase on Frame C.

Based on the above idealization a numerical analysis using the constant velocity recurrence formulation given by Biggs [4] was made. The appendix gives an explanation of the analysis and a sample program printout.

Although there are problems with inelastic and limit design of reinforced concrete structures due mainly to working load serviceability, moment redistribution and negative stiffness under static loads [22] and [19]; plastic analysis for dynamic loads of limited energy capacity and rare occurence should prove more acceptable. Particularly, an elasto-plastic or stiffness degrading analysis of a ductile reinforced concrete frame may be useful when its natural frequency is low with respect to the frequency of the dynamic force so that plastic action may be short in time and displacement.

5.2 Static Frame Analysis.

In order to provide a check on observed results from the static Frame C and, to estimate the strain rate during the rise period of the impact a standard elastic and plastic frame analysis was made.

The plastic analysis assumed that the moment rotation characteristics of the hinges were elasto-plastic. This does not agree with the observed hinge formation in Joint 2 (see Section 4.7). Cohn [21] gives us a fundamental condition for limit design in reinforced concrete structures that rotation compatibility be maintained, that each hinge in a mechanism develop its full plastic capacity without premature local failure. However, as mentioned in Section 4.7 improved detailing might well develop a full plastic hinge in this joint. Based on the lateral sidesway mechanism with column hinges assuming full yield moment at all joints and the concrete properties for Frame C the lateral yield load was calculated. The column section yield moment and maximum concrete stress at yield was calculated after Mattock [13]. Centerline dimensions were used for the structure and axial load was neglected. These calculations showed a lateral yield load of 1.03 Kips c.f. 1.1 Kips observed in first loading of Frame C.

The frame was analysed elastically to compare initial stiffness using centre line dimensions, Frame C properties and ignoring axial load. The stiffness of the frame was calculated from the slope deflection equations and the moments of inertia of the concrete cross sections based on reference [14] recommendations taking the transformed cracked sections. The beam moment of inertia was taken as the simple average for positive bending at one end and negative at the other end of the beam. This calculation gave a lateral stiffness of 10.75 Kips per inch c.f. 10.4 Kips per inch observed for the linearized first loading curve of Frame C. This appears to be a good comparison considering the stiffness of the elements is probably less than assumed since between cracks the concrete will take tension.

VI. DISCUSSION.

6.1 Test Results.

The frequency of the free vibration for Tests A-1 to A-30 dropped from 12.5 Hertz to 11.04 Hertz as shown in Table 2. The decrease in frequency from Tests A-1 to A-20 at peak impact force of 900 pounds was 8%, with nearly all of this decrease occuring in the first four tests. The first three tests response records were irregular and difficult to interpret. From Tests A-21 to A-30 at the higher peak impact force of 1200 pounds the frequency dropped 4% in much the same pattern observed in the previous impacts. The natural frequency of the final tests at a fixed peak impact force appeared to approach a steady value more so for the second series than for the first.

The logarithmic decrement of the free response remains about the same after repeated impulses with the same peak force. Average values of .16 for Test A-10 to A-20 and .2 for Test A-21 to A-30 are evident from Table 2.

The amplitude of the free vibration is less in the early tests at a given impact than it is during later tests. Figure 15 shows the plot,number of impulses at or below a particular level versus amplitude of the first peak of response. The trend for Test A-1 to A-20 shows A_1 has increased 3.6 times. Tests A-20 to A-30 are plotted on Figure 15 as well; although they have a prior history of Tests A-1 to A-20 and show A_1 increasing by 41% during these impacts.

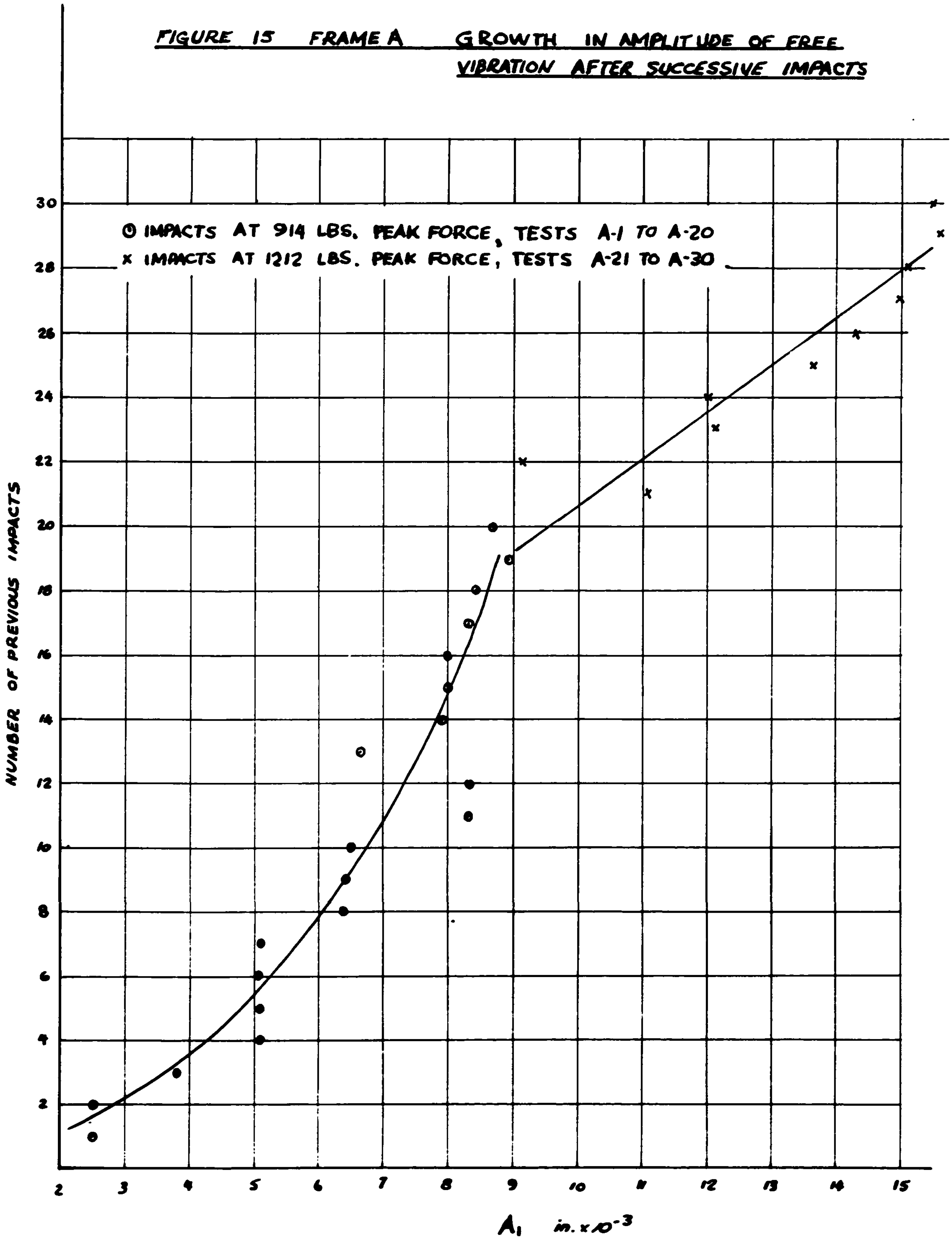
FIGURE 15 FRAME A GROWTH IN AMPLITUDE OF FREE VIBRATION AFTER SUCCESSIVE IMPACTS
⊙ IMPACTS AT 914 LBS. PEAK FORCE, TESTS A-1 TO A-20
× IMPACTS AT 1212 LBS. PEAK FORCE, TESTS A-21 TO A-30
NUMBER OF PREVIOUS IMPACTS
A1 in. × 10^-3
2
4
6
8
10
12
14
16
18
20
22
24
26
28
30
3
5
7
9
11
13
15

Table 2 shows significant plastic deformation in the first three tests on Frame A, Tests A-1 to A-20. However, for Tests A-20 to A-30 the plastic deformation is more evenly distributed throughout the tests.

Bate [9] commenting on reinforced concrete beams subjected to repeated loading says, "When the range of repeated loading is larger (than maximum load not exceeding half cracking load) but within the limiting range, cracking and permanent deformation increase with increasing numbers of repitions of load until a condition of stability is reached. At this stage, the dynamic deformation is almost elastic, and no further increase in the size of the cracks take place." This elasticizing of the deflection curve and the implication that there would be less hysteristic energy dissipation on later than on earlier tests might reflect on the increase in A_1 which can represent energy transmitted to the free vibration response.

This might be explained in there being a certain amount of the frames internal energy dissipative capacity that is amplitude dependent, such as flexural cracking, and after a number of repeated impacts at the same peak force level is exhausted. This type of damping is not likely to be evident in the free vibrations logarithmic decrement due to the relatively low amplitudes compared to the maximum forced vibration amplitude. This is indicated in the fact the logarithmic decrement did not change significantly for impacts at the same peak force in Frame A tests. Figure 22 indicates a considerable energy absorption on the first impact loading of Frame B compared to later tests.

It might be suspected that the stiffness of the frame deteriorated rapidly in the first few impacts at the same peak force and then assumed a steady value as reflected in the natural frequency behaviour.

It would appear from the final tests on Frame A and Tests on Frame E after the first attempt at E-11 that the previous impacts had caused extensive damage which affected the frames resistance during subsequent tests. After twenty impacts at 900 pounds, and ten at 1200 pounds peak force on Frame A, the next impact at 1540 pounds maximum and a long flat top resulted in one inch, permanent sidesway deformation. Frame B withstood impacts of higher peak forces and less deformation from Test B-9 to the final Test B-14.

Frame B (Figure 16) and E (Figure 19) show similar behaviour with respect to decreasing natural frequency and increasing logarithmic decrement due to successively increasing lateral impacts.

Figure 16 shows the natural frequency of free vibration decreasing with increasing impact peak force. This decrease is relatively small for the peak loads which would not result in large plastic deformations but for higher impact loads, above the ultimate static strength of the frame, this decrease is much greater. The total change ranges from 13.3 Hertz under 420 pounds peak force to 9.04 Hertz at 1750 pounds peak force, a 32% drop.

The average frequencies for Frame A Tests A-1 to A-20 and A-20 to A-30 were plotted on Figure 16 and fall at a lower frequency than the test displayed by Frame B results. This indicates the effect repeated impacts at the Frame A tests load levels has on the natural frequency of the frame. As a check on this observation the frequency for Test A-1

FIGURE 16 FRAME B PEAK IMPACT FORCE vs NATURAL FREQUENCY & LOGARITHMIC DECREMENT

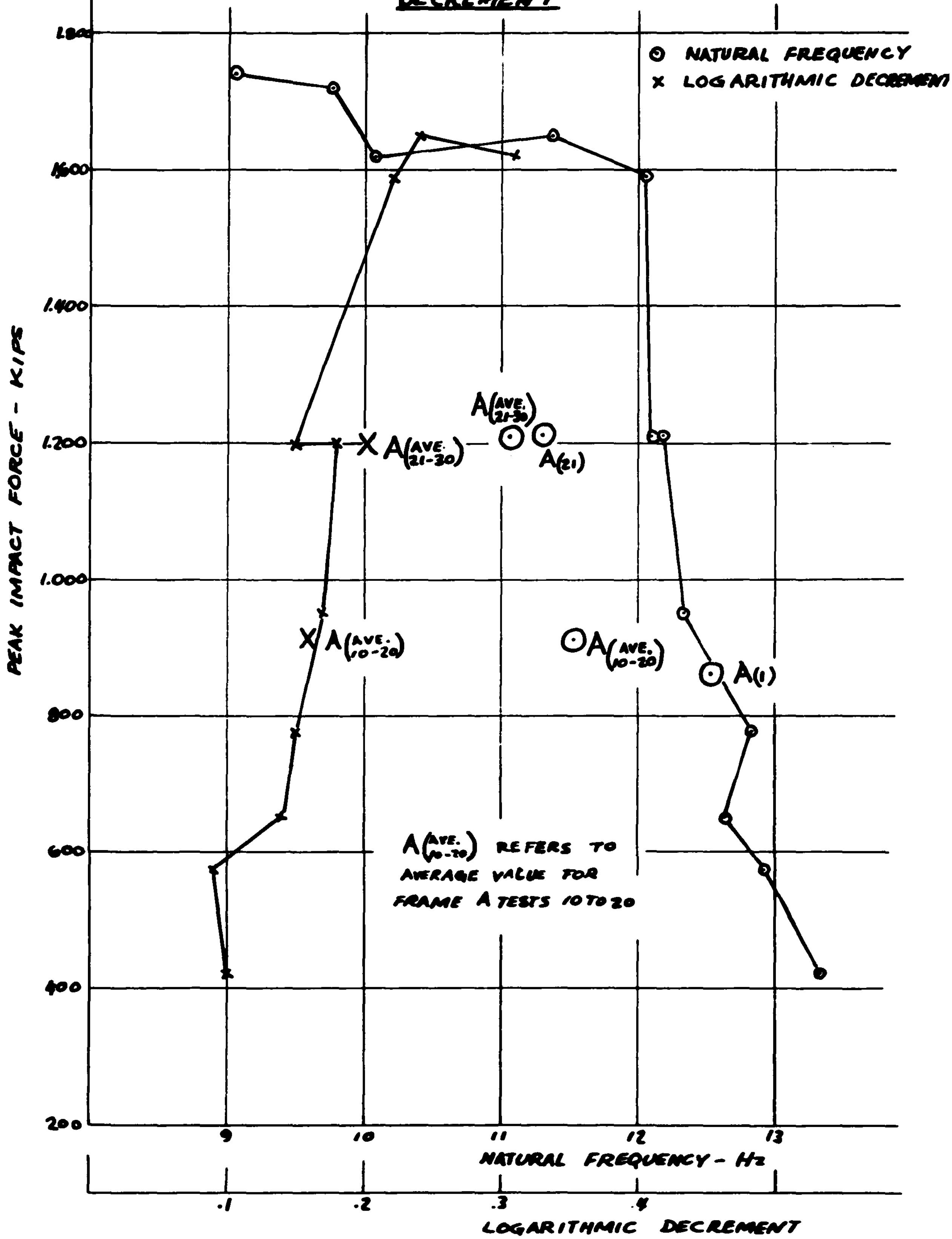

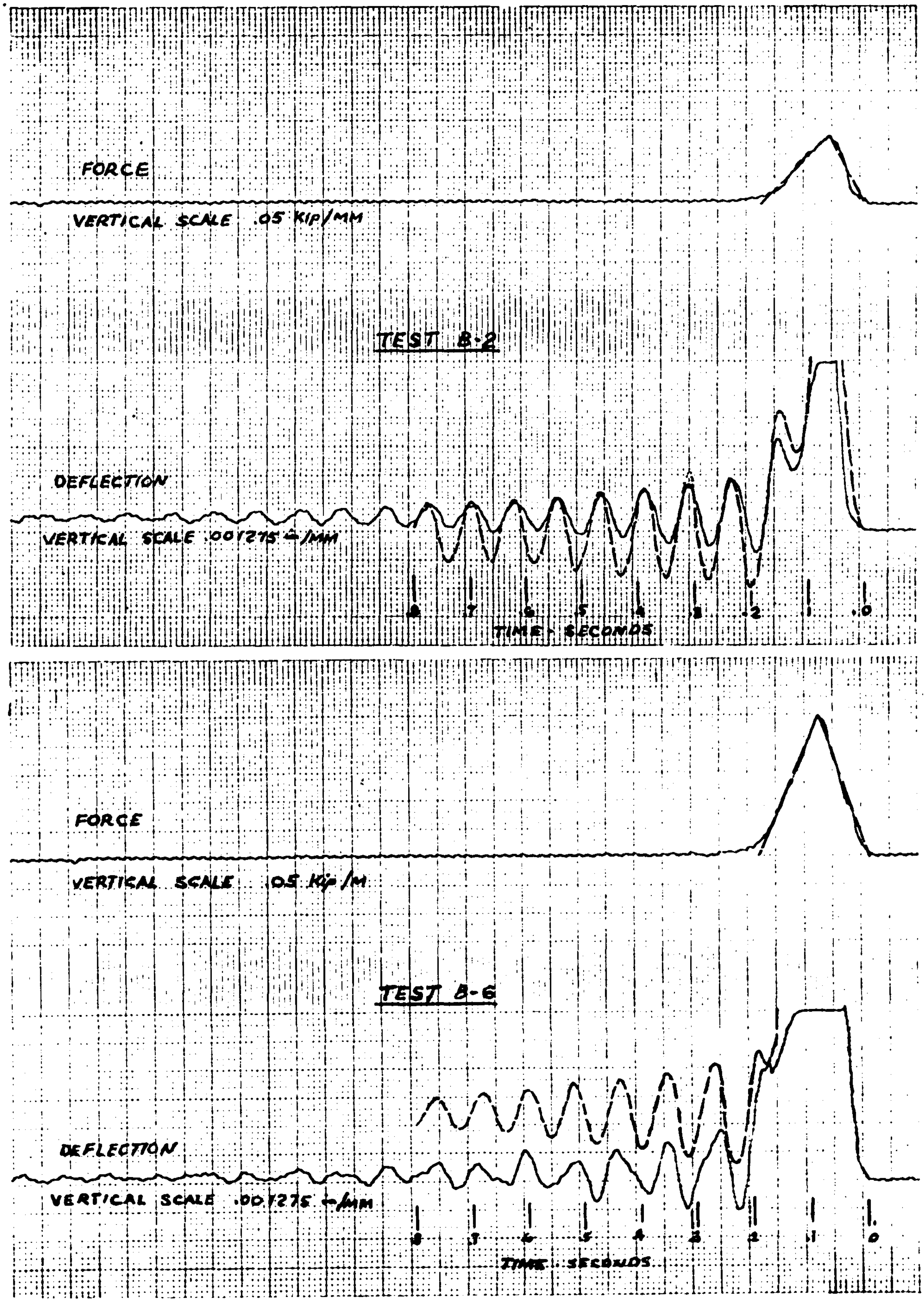

DASHED LINES - CALCULATED OR LINERIZED
SOLID LINES - OBSERVED

FIGURE 17 CALCULATED & OBSERVED RESPONSE FOR TESTS B-2 & B-6

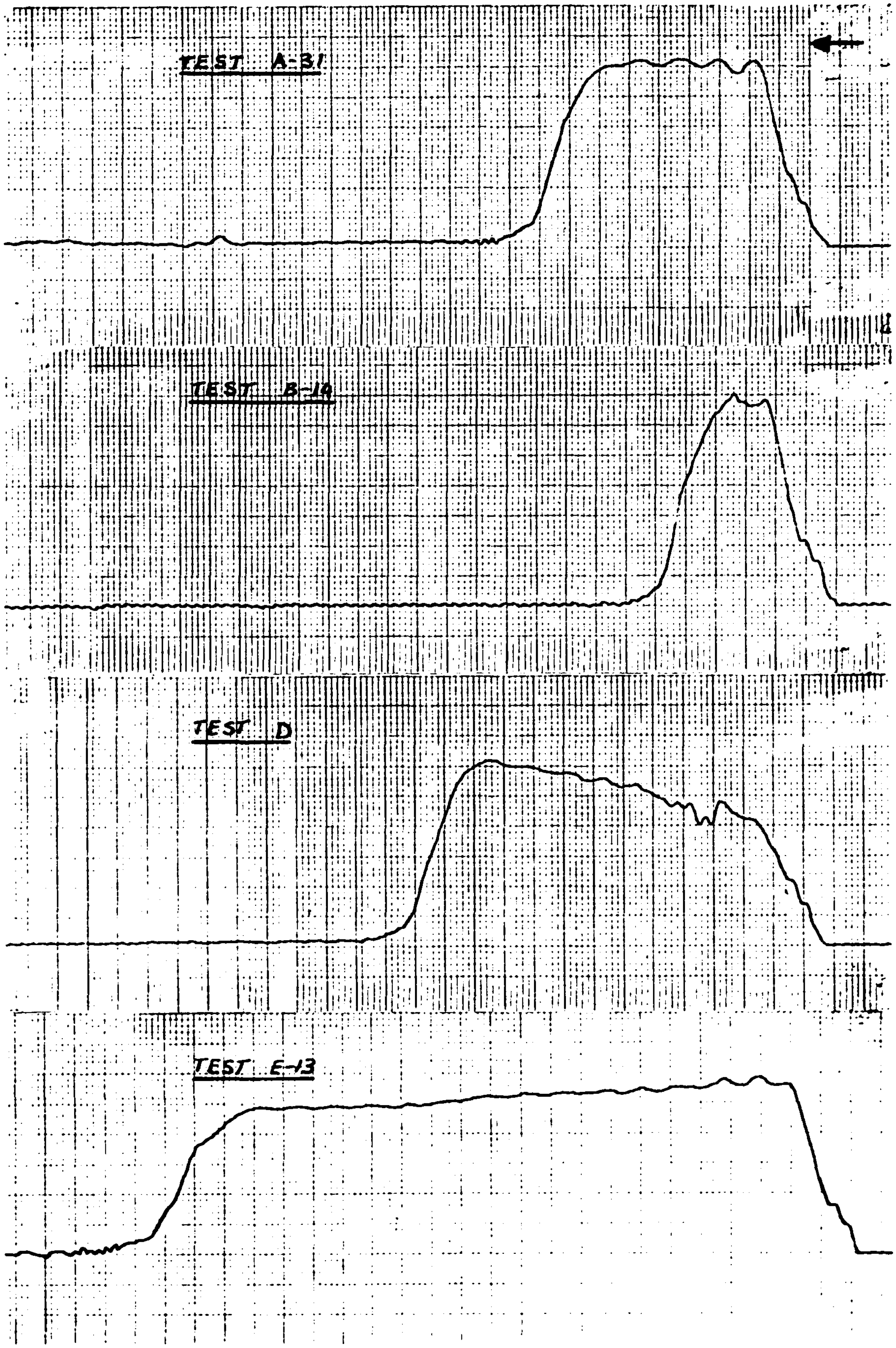

SCALES: HORIZONTAL . SEC. = 1MM , VERTICAL .05 K = 1MM

FIGURE 18 IMPACTS OF FINAL TESTS

FIGURE 19 FRAME E PEAK IMPACT FORCE vs. NATURAL FREQUENCY & LOGARITHMIC DECREMENT

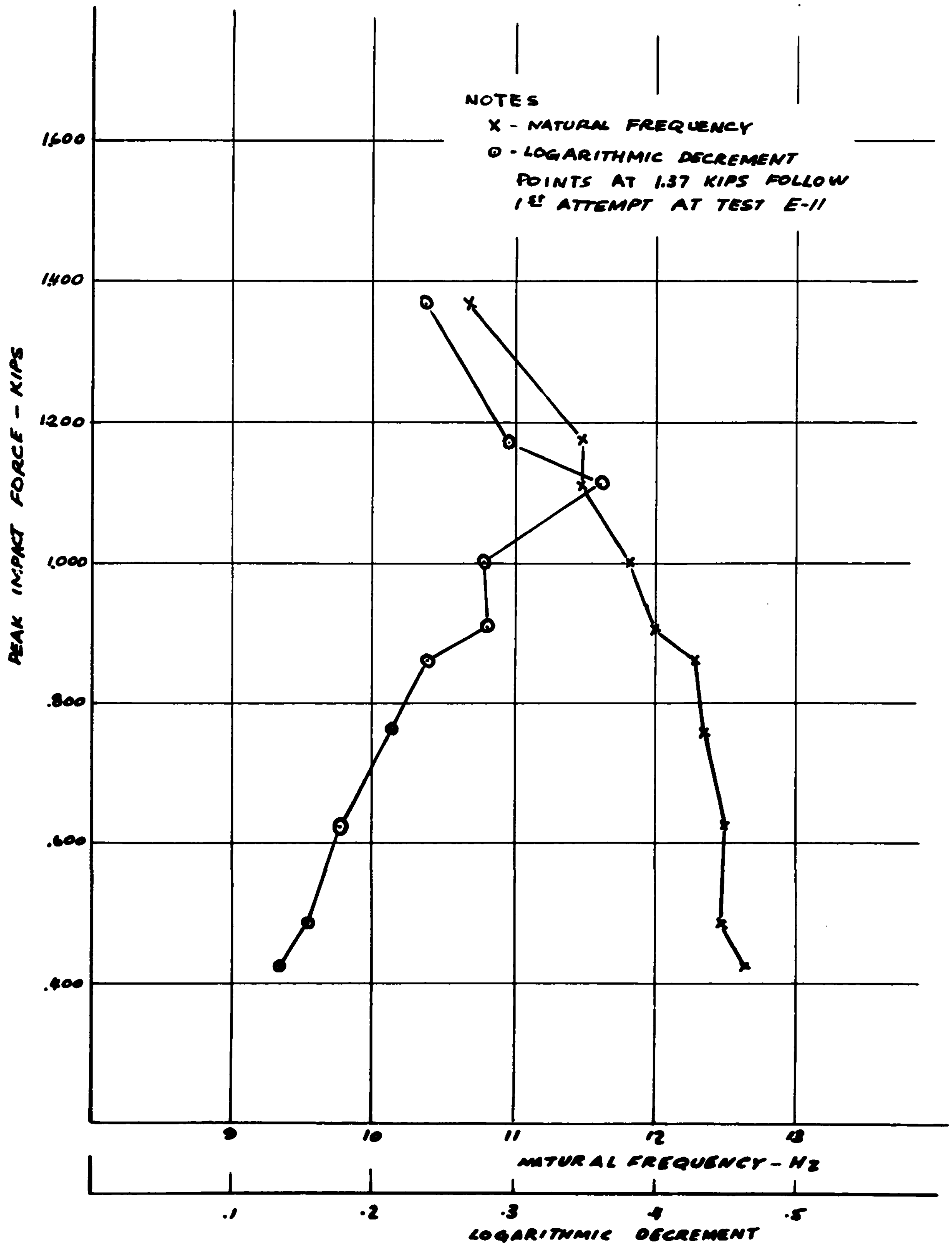

and A-21, the first tests in the respective impact series for Frame A were also plotted on Figure 16. The A-1 test point falls very close to the trend and the Test A-21 point falls between the trend and the average of Tests A-21 to A-30, as might be expected.

The general tendency of the logarithmic decrement is to increase with increasing peak impact load as shown in Figure 16 and 19. Although the individual points on this plot show a wide dispersion the trend would indicate a twofold increase in the logarithmic decrement between 400 pounds and 1600 pounds peak impact force. This indicates a greater equivalent viscous damping after successively higher impacts. Expressed as a percentage of critical damping, values ranged from 1.6% at 420 pounds peak force to 4.9% at 1650 pounds peak force for B tests.

Calculated and observed responses, for peak impact force below the lateral yield load of the frame, agree fairly well. The table below compares the calculated and observed maximum forced response for the first tests on Frames A, B and C.

FRAME - TEST	OBSERVED	CALCULATED
A-1	.089 inches	.0818 inches
B-1	.035 inches	.0395 inches
E-1	.0386 inches	.0509 inches

Figure 17 shows the records of Test B-2 and B-6 with the calculated response and linearized impulse superimposed. The calculated response for B-2 remained elastic while the observed response showed quite a bit of residual deformation. The calculated response for Test B-6 was elasto-plastic and showed much more plastic deformation than was actually observed. From Tests B-7 to B-14 the calculation grossly over-estimated permanent plastic deformations. As well, the calculations generally over-estimated the amplitude of free vibrations in all the tests for which a comparison could be made. Tests B-8 to B-10 showed a much more irregular free vibration response with amplitudes decreasing abruptly from previous tests. Test B-8 coincided with the observation of hairline cracks in hinges 1 and 3, as well, from B-8 onward the residual plastic deformation increased considerably over previous values as can be seen in Table 3.

6.2 Calculated & Observed Response for Tests A-23 & B-12.

Calculated responses for Frame B tests above Test B-6 with maximum frame resistance of 1100 pounds consistently indicated larger deflections; maximum forced deflection, residual plastic deformation, and the amplitude of free vibration was greater than observed. This higher deflection resistance of the actual frame compared to the elasto-plastic prompted a comparison of calculated response with increased frame yield resistance, Q, to the observed response for Tests A-23 and B-12.

Figures 20 and 21 show the observed response and calculated response for Frames A-23 and B-12 respectively.

For a yield frame resistance of 1100 pounds obtained from the static test both the residual plastic deformation and the maximum response for the calculated model are greatly over-estimated. However, if Q is increased to 1175 pounds for Test A-23 and 1400 pounds for Test B-12 we get a closer agreement between observed and calculated maximum displacement and residual plastic deformation. The increased

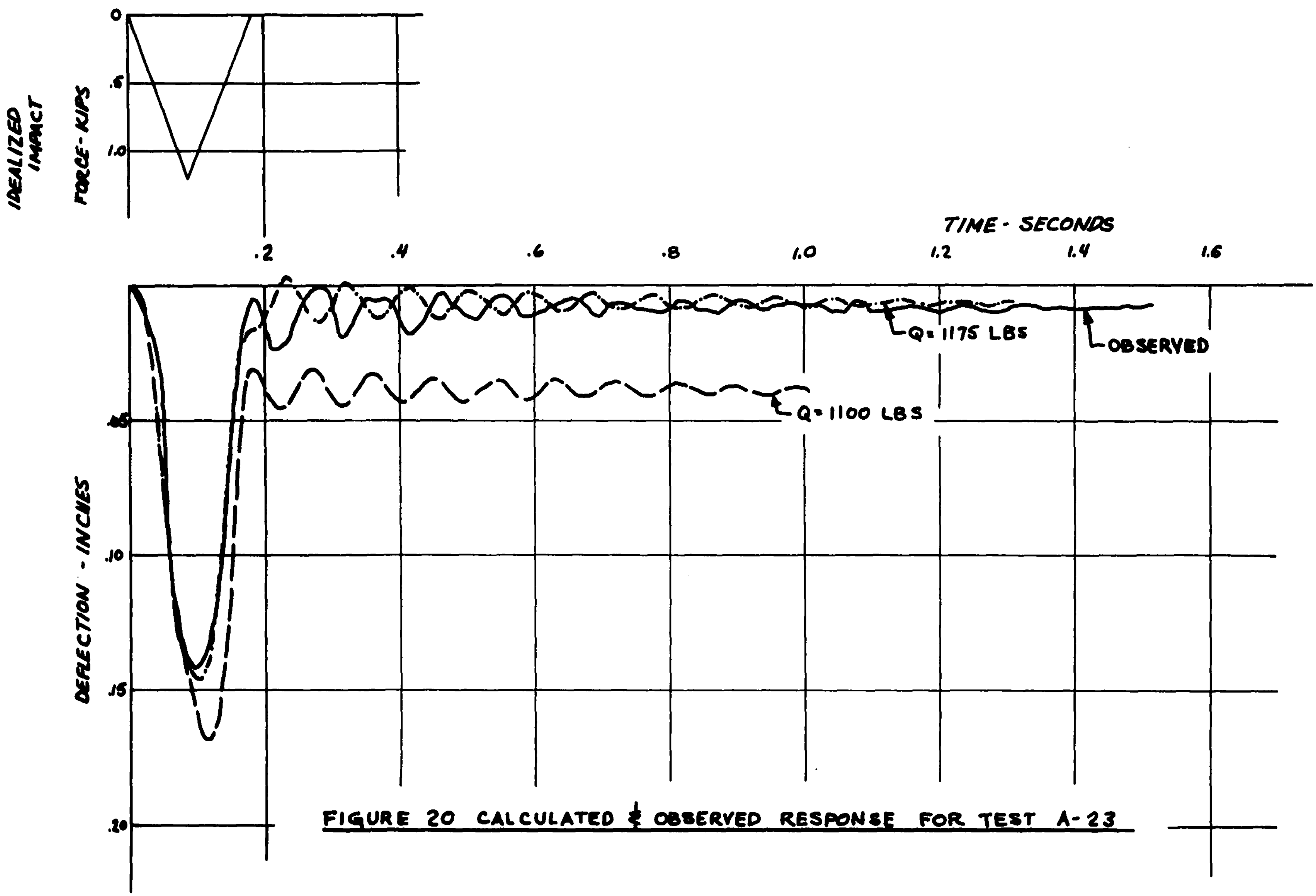

FIGURE 20 CALCULATED & OBSERVED RESPONSE FOR TEST A-23

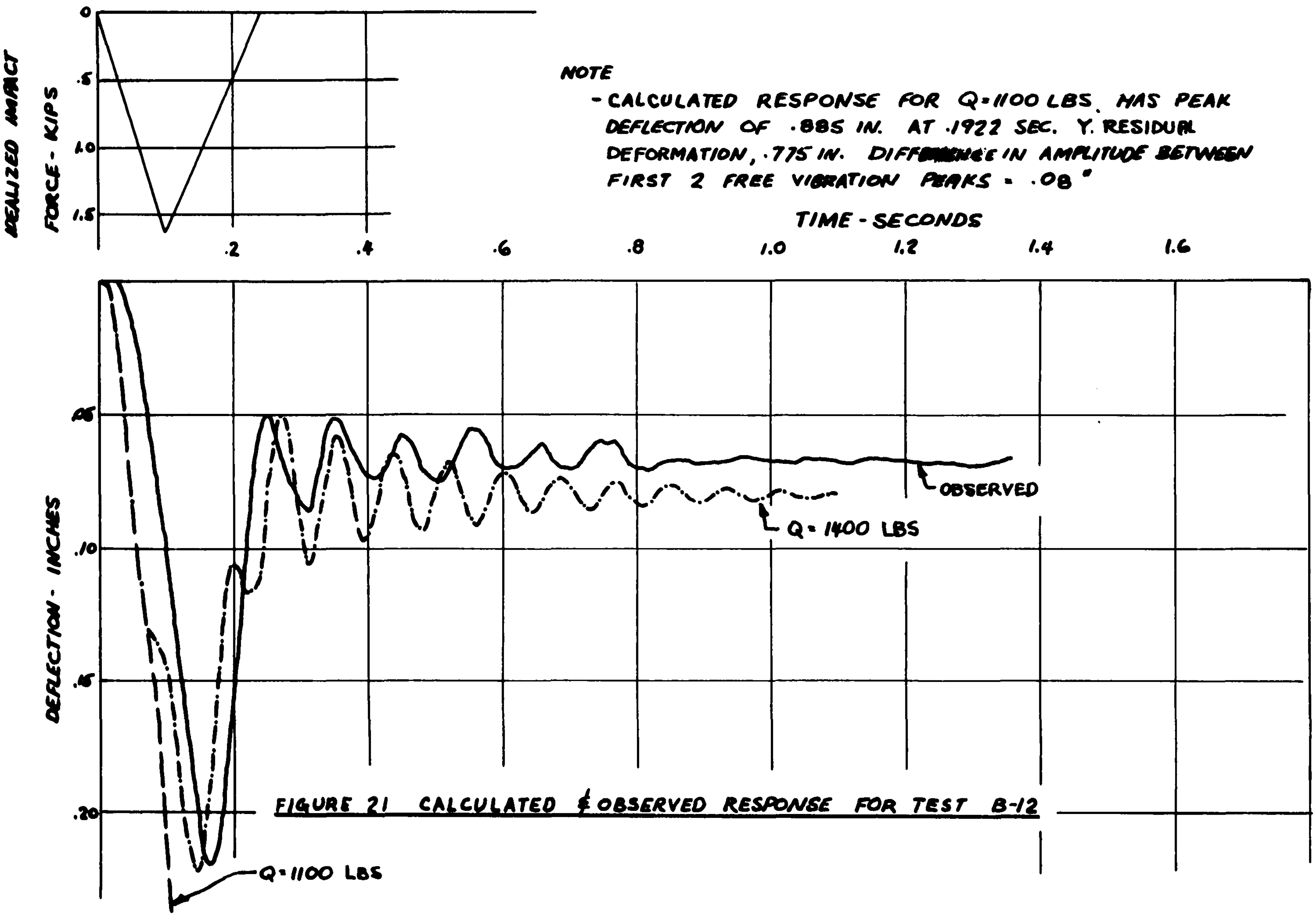

FIGURE 21 CALCULATED & OBSERVED RESPONSE FOR TEST B-12

apparent frame resistance brings the plastic work dissipated by the mathematical model more in line with that of the actual frame (based on a static yield resistance of 1100 pounds times the permanent deformation) as shown in the table below.

DISTORTION ENERGY (PLASTIC WORK) pounds-inches	A-23	B-12
Actual Frame	-8.8	-73.7
Calculated (Increased Q)	-7.42	-112.08
Calculated (Q=1100 lbs.)	-24.83	-851.97

Increasing the frame's yield resistance in the mathematical model does not improve the shape of the response curve itself. In fact, the free vibration has a 180° phase shift from the observed as well as the forced response, except for its height is not improved for B-12. This is mainly because the mathematical model does not consider the actual non-linear force deflection characteristic energy dissipation beyond that which can be expressed as equivalent viscous or plastic work as well as the actual impulse applied.

To check the effect of over-estimating the recorded impulse, which is discussed in Section 6.4, the calculations for Test A-23 and B-12 were repeated with a yield frame resistance of 1100 pounds, and a negligible decay time for the impulse (TI = TR + .0001 seconds). This analysis showed the calculations still over-estimated the maximum response permanent deformation and distortion energy.

The apparent increase in strength may be due in part to the strain hardening exhibited in the static load tests after the lateral yield load was reached. Based on the accumulated plastic residual deflections before Tests A-23 and B-12, assuming the initial loading curve, Figure 15, will behave in an elasto-plastic manner, the new lateral frame yield resistances are estimated as 1120 pounds for A-23 and 1160 pounds for B-12.

This analysis although rather crude and qualitative indicates the frames had a higher apparent strength under impact load than under static load.

Liu [15] comparing accumulated damage of elasto-plastic and stiffness degrading systems in an analytical study of a single mode oscillator subjected to simulated ground motion finds, "That the damage accumulation for stiffness degrading systems is not so severe as corresponding elasto-plastic systems" and attributes this to the higher internal energy dissipation capability of the stiffness degrading system.

6.3 Rate of Straining Effects.

The concrete strain rate was calculated from the average (over the rise time) of the first ten tests on Frame A, the elastic analysis maximum concrete bending stress (lateral load only) to lateral load ratio, and the stress strain curve for Frame C concrete, Figure 10, to be .0078 inches per inch per second. Watstein [20] observed an increase in the dynamic secant modulus of elasticity of plain 3 inch x 6 inch concrete cylinders under increasing strain rate. His results would indicate a ratio of static to dynamic moduli of 1.07 for these tests. This effect would tend to reduce the above calculated strain rate in the same proportion since it was based on a static stress strain curve. Dilger's [5] results for rapidly applied loads to confined prisms with a steel percentage of 1.6% show an increase in ultimate stress of 40% to 57% over an essentially static strength between .004 inches per inch per second and .067 inches per inch per second.

As steel yielding progresses, the concrete compression area decreases until the concrete fails in crushing. It is during this phase that the increased strength of concrete under high strain rates may increase the moment capacity by increasing the compressive force and shifting the centroid of compressive stress closer to the compressive face increasing the internal moment arm. Tensile mechanisms acting to increase the strength may be an increased stiffness of the tensile reinforcement - cracked concrete zone as well as increased yield strength of steel under high strain rates.

Dilger [5] also observed that the ductility of confined concrete is independent of strain rate and beyond a concrete strain of approximately .007 inches per inch the ultimate stress versus strain curves for varying strain rates coincide, indicating for large hinge rotations there may not be an appreciable increase in energy absorption due to high strain rate.

6.4 Experimental Technique.

The rates of initial loading obtained in these tests require that the Gilmore force pulse system was used at its capacity. It was evident from those tests in which there was substantial yielding and low stiffness in the frame that the hydraulic ram did not react fast enough to exert a triangular force pulse and the rather flat-topped impacts of Figure 18 resulted.

Figure 22 is a plot of load cell versus LVDT readings for the duration of the force pulse. The area contained between the rising and falling portions of this curve represent the work input into the frame minus an allowance for the inertia force on the frame and friction between the electromagnet chair and its support post. This area decreases for successive impacts at the same peak load and is negative for Tests A-8 and A-10 appearing to violate the Law of Conservation of Energy.

This result is most likely due to the friction forces between magnet chair and support during the force decay period of the impact when the load cell would measure these forces as well as the frame resistance but, the LVDT only measures the frame displacement.

These effects tend to over-estimate the actual force on the frame during the decay period and this portion of the impact cannot be considered reliable data. The actual force on the frame would better have been measured with a load cell between the pull-off plate and the frame.

It might be expected from the response of Frame A Tests A-1 to A-10 (see Section 4.2) that energy dissipation during one test in a series at the same peak load decreases from previous tests. This impression could not be adequately sustained or disproved from an energy balance point of view, as the energy losses in the apparatus were not evaluated or isolated.

The problem of energy loss to the base beam could be almost eliminated with a massive rigid foundation for the apparatus and better attachment and clamping details might

FIGURE 22 FRAME A LOAD CELL vs LVDT CURVES

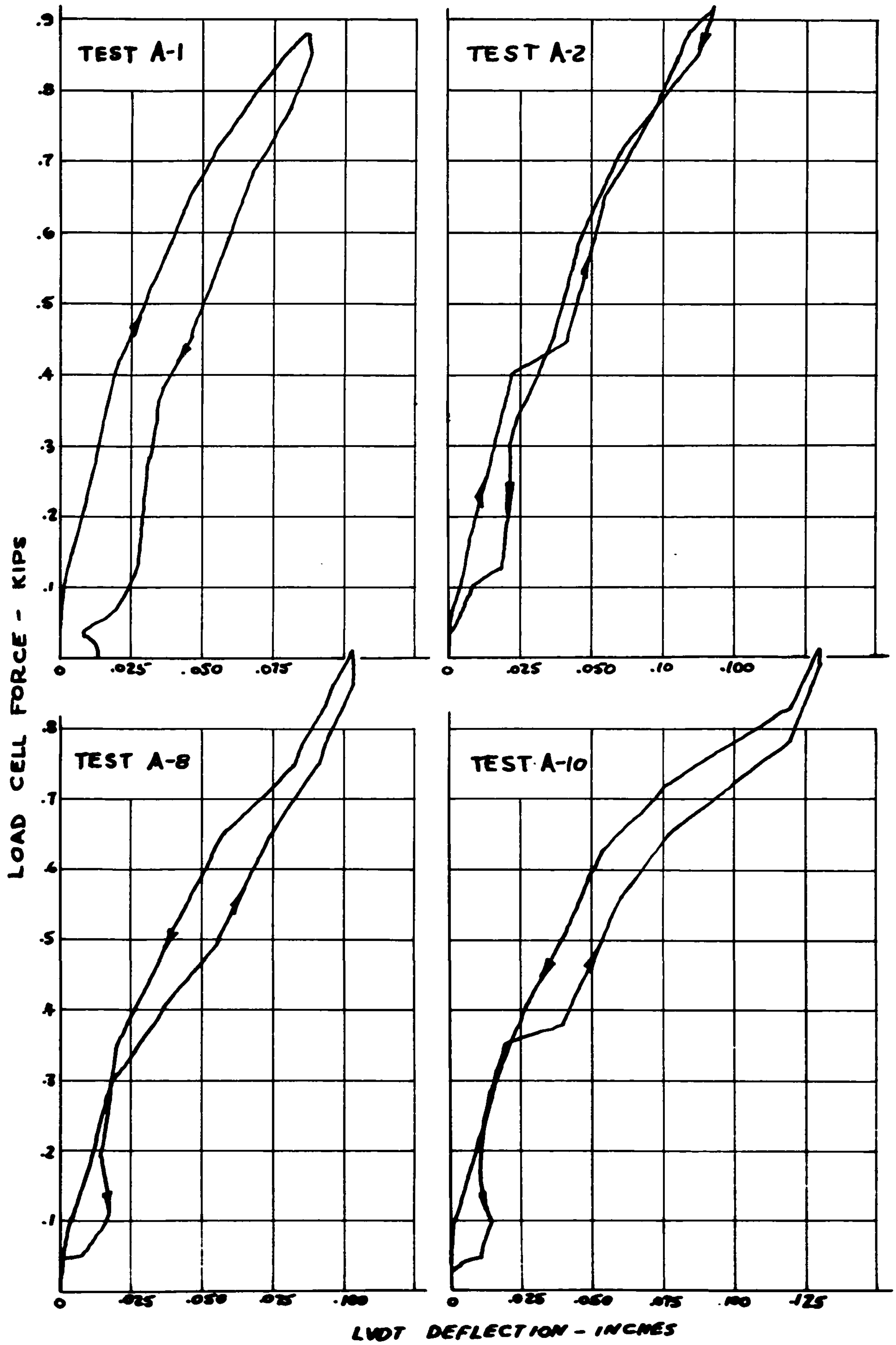

reduce specimen-apparatus interface shock and crushing losses if this proved to be a problem.

VII. CLOSURE.

7.1 Conclusions.

Repeated lateral impacts of the same peak force acting at beam level on a model reinforced concrete portal frame bring about an increase in the amplitude of free vibration above initial values. This increase in amplitude response, measured as the height above the residual plastic deformation, was about two times for the series of impacts at 900 pounds and only 50% for the series at 1200 pounds peak force.

The frequency of the free vibration response to repeated impacts at the same peak force decreases while the logarithmic decrement does not change significantly. The decrease in observed natural frequencies of the first twenty tests on Frame A was 8% while the decrease for the next ten tests at a higher impact was 4%. All of this decrease occurred in the first few tests of the series.

As evidenced by Frames A and E (after the first attempt Test E-11) inability to sustain the high impact peak forces applied to Frame B, the effect of repeated impacts on the frame reduces its resistance to impacts at higher peak force levels and points to a deterioration of the structure under these repeated impacts.

Successively higher impacts on the frames caused a decrease in the natural frequency of free response and an increase in the logarithmic decrement. For the impacts used in Frame B, a 32% decrease in frequency was observed and the logarithmic decrement trend increased twofold from the first to the twelfth impact although individual points showed a wide dispersion. This points to the problem of choosing a suitable viscous damping coefficient for analysis of a reinforced concrete structure to earthquake where the structures previous seismic history would be a great influence.

The calculated elasto-plastic model based on the static lateral yield load gives a fair indication of response to impact for low peak forces, below the static value, but greatly over-estimates response to high impacts. The effect of reversed loading (Frame D), the apparent increase in strength, and the poor comparison of the elastoplastic model and observed responses to high peak impact forces point out the need of a history dependent, stiffness decaying & strain rate sensitive mathematical model to effectively describe response to these loads.

The frames showed a greater resistance to impact load than would be expected from the static force deflection relationship and elastoplastic analysis. Test A-23 showed a 7% and Test B-12 a 27% increase in apparent resistance over the static value measured as an equivalent lateral frame yield resistance. The overestimation of deflection response of the elasto-plastic analysis based on static strength indicates neglect of the apparent strength increase is conservative.

Notwithstanding the probable abrupt failure of joint 2, the frames showed a reserve plastic deformation capacity and the development of ductile hinges under impact. Detailing for ductile hinge formation at the column-beam joint may well have improved the frame resistance.

The experimental technique and model require refinement if future tests are to gain a more quantitative evaluation of dynamic behaviour and obtain better control over the prescribed force pulse.

7.2 Future Investigation

Using the same model with a periodic forcing function, resonance tests might yield useful damping and non-linear response information.

An analysis of the frame based on a stiffness degrading mathematical model as suggested in [15] and [3] may give a better indication of the observed impact response.

Impact response of frames having past histories of reversed plasticity might be studied; a particular question being whether these frames can evoke an increased resistance over the static value.

Further impact studies using the present technique should consider the problems brought out in Section 6.4 and more sophisticated instrumentation.

VIII. REFERENCES

References 1 and [16] contain many excellent references on this topic in their bibliographies.

1. Liebich, L.J., "Dynamic Loading of Small Concrete Structures", M. Eng. Thesis McGill University, Montreal, 1968.

2. Blume, Newmark & Corning. "Design of Multistory Reinforced Concrete Buildings for Earthquake Motions". PCA, 1961, Skokie, Illinois.

3. Takeda, Sozen & Nielsen, "Reinforced Concrete Response to Simulated Earthquakes", Proceedings ASCE, Str. Div., ST12, Dec. 1970.

4. Biggs, "Introduction to Structural Dynamics", McGraw Hill, New York.

5. Dil ger, "Report to EMO, Oct. 1970, Ultimate Strength of Statically Indeterminant Reinforced Concrete Structures".

6. Watstein, D., "Effect of Straining Rate on the Compressive Strength and Elastic Properties of Concrete", Journal ACI, April 1953, Vol.24.

7. Blume, J.A., "Design of Earthquake-Resistant Poured-in-Place Concrete Structures" published in <u>Earthquake Engineering</u>, R.L. Weigel, coordinating editor, Prentice Hall Inc., 1970.

8. Sabnis & White, "Behaviour of Reinforced Concrete Frames Under Cyclic Loads Using Small Scale Models", Journal ACI, Sept., 1969.

9. Bate, S.C.C., "The Strength of Concrete Members Under Dynamic Loading", <u>A Symposium on the Strength of Concrete Structures</u>, Cement and Concrete Association, London, May 1956.

10. Borges, J.F. and Pereira, Jervis, "Dynamic Model Studies for Designing Concrete Structures", <u>Models for Concrete Structures</u>, ACI Publication SP-24, Detroit, 1970.

11. Aldridge, W.W. and Breen, J.E., "Useful techniques in Direct Modelling of Reinforced Concrete Structures", <u>Models for Concrete Structures</u>, ACI Publication SP-24, Detroit, 1970.

REFERENCES (cont'd)

12. Zia, P., White, Richard, Vanhorne D., "Principles of Model Analysis", Models for Concrete Structures, ACI Publication SP-24

13. Mattock, A.H., "Rotational Capacity of Hinging Regions in Reinforced Concrete Beams", Flexural Mechanics of Reinforced Concrete, ACI SP-12, 1964.

14. ACI-318-63, "Building Code Requirements for Reinforced Concrete", 1963.

15. Liu Shih-Chi, "Earthquake Response Statistics of Non-linear Systems", Journal ASCE, EM2, April, 1969.

16. Symposium on Earthquake Engineering, University of British Columbia, Vancouver, B.C., Sept., 1965.

17. Sader, W.H., "Ultimate Strength of Single Bay One Story Reinforced Concrete Frames Subjected to Horizontal and Vertical Loadings." M. Eng. thesis, McGill University, Montreal, 1967.

19. Winter, G., "Whither Inelastic Concrete Design?", ACI SP-12, 1964.

20. Watstein, D., "Effect of Straining Rate on the Compressive Strength and Elastic Properties of Concrete", Journal ACI, April, 1953.

21. Cohn, M.Z., "Rotation Compatibility in the Limit Design of Reinforced Concrete Continuous Beams", ACI SP-12, 1964.

22. Rosenblueth, E., and de Cassio, R.D., "Instability Considerations in Limit Design of Concrete Frames", ACI SP-12, 1964.

23. Tsui, H. and Mirza, M.S., "Model Microconcrete Mixes Structural Concrete Series No. 23", Nov. 1969, Dept. Civil Engineering and Applied Mechanics, McGill University, Montreal.

24. Watson, A., "Energy Absorption of Model Beams Under Impact Loads", M. Eng. thesis, McGill University, 1967.

PCA = Portland Cement Association
ASCE = American Scoiety of Civil Engineers
ACI = American Concrete Institute

APPENDIX: Response Analysis.

The numerical analysis of the frame response was based on the constant velocity recurrence formulation outlined by Biggs [4]. The problem was programmed for solution on McGill's IBM 360/70 computer a typical printout and list of symbols follow. The mathematical idealization is given below.

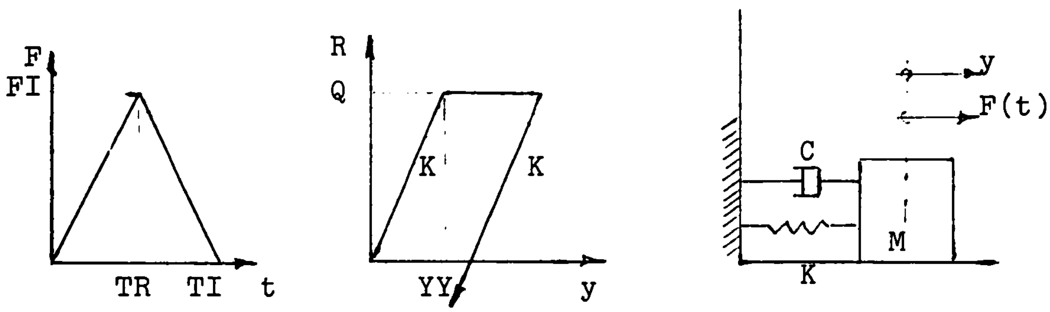

FORCE PULSE — FRAME RESISTANCE CHARACTERISTIC — MODEL

Using the constant velocity formulation it is necessary to have the displacement from the beginning of the previous interval which is nonexistant for the first interval. A closed form solution for the displacement was obtained at the end of the first interval based on the following equation of motion and initial conditions, assuming elastic response.

$$M\ddot{y} + c\dot{y} + Ky = \frac{FI}{TR}\, t$$

Initial conditions $\dot{y} = y = 0$ @ $t = 0$

It can readily be shown [4] the solution of this equation is.

$$y = \frac{FI}{TR}\left[e^{-Bt}\left(-\frac{1}{Wd}\left(B\frac{C}{K^2} + \frac{1}{K}\right)\sin W_d t + \frac{C}{K^2}\cos W_d t\right) - \frac{C}{K^2} + \frac{t}{K}\right]$$

where

C = coefficient of viscous damping

K = frame stiffness

t = time

M = mass

$B = C/2M$

$W_d = \sqrt{W^2 - B^2}$

$W = \sqrt{K/M}$

y = displacement and dots represent time derivatives.

Biggs [4] gives the recurrance formula:

$$Ye = 2Y_B - Y_F + \ddot{Y}_B (DT)^2$$

where

Ye = displacement at end of interval.

Y_B = displacement at beginning of interval.

Y_F = displacement at beginning of the former interval.

$\ddot{Y}_B$ = acceleration at the beginning of the interval calculated from the equation of motion.

DT = the numerical integration time interval.

An energy balance was made at the end of the force pulse and might serve as an indication of the accuracy of the numerical integration to that point.

The energy due to damping was calculated by summing up dissipated energy over an interval DT assuming a linear velocity distribution and taking the average velocity in the interval.

$$dD = -C\, V_{AVE}\, dY.$$

where

dD = incremental energy dissipation

V_{AVE} = average velocity over the interval.

The input work done was calculated using Simpson's rule in two stages, $0 \leq T \leq TR$ and $TR \leq T \leq TI$, with F, the applied force, used as the independent variable. Assuming there are an even number of time, and so force, increments in each stage and that the initial displacement for the first stage is zero the work done will be the negative of the area between the rising and falling stages which is also the total complimentary energy.

So, first stage complementary energy,

$$CEI = \frac{FI \times DT}{TR \times 3} [4Y_{DT} + 2Y_{2DT} \cdots 4Y_{TR-DT} + Y_{TR}]$$

Second stage complimentary energy,

$$CEO = \frac{FI \times DT}{(TR - TI) \times 3} [Y_{TR} + 4Y_{TR + DT} + 2Y_{TR + 2DT} \cdots$$

$$4Y_{TI - DT} + Y_{TI}]$$

$$WORK = -(CEI + CEO)$$

The other energy calculations are self-explanatory from the programme printout.

NOTES ON PROGRAM

1.) DT, integration interval has to be less than one-tenth the natural period of the structure.

2.) The first interval is assumed elastic.

3.) Rebound is assumed not to extend into a negative plastic region.

4.) At time t = 0, y = 0, y = 0, y = 0, plastic yield = 0.

5.) Basic dimensions pounds, seconds and inches.

6.) Program assumes that the iteration interval is always half times the storage interval.

7.) Program calculates deflection at the end of an interval from initial and former values and does not recalculate or interpolate deflections if a discontinuity occurs during that interval e.g. for the forcing function as the frame resistance moving from an elastic to a plastic region. This will cause negligible error if the interval, DT, is taken small enough.

8.) Trapezoidal rule was used to calculate damped work and Simpson's rule was used to calculate net input work. TR/DT and (TI - TR)/DT must be even for Simpson's rule integrations. (TR - TI) must be greater than zero. This is required only for the energy balance calculations and not for the response.

PROGRAM NOTATION

NFMS	- Number of frame tests = Number of data cards.
FRM	- Frame
IST	- Test
FI	- Peak impulse force, pounds.
TR	- Impulse rise time, seconds.
TI	- Total impulse time, seconds.
K	- Stiffness, pounds per inch.
Q	- Frame yield resistance.
PD	- Ratio of critical damping.
M	- Mass, pounds seconds^2 per inch.
DT	- Integration interval, seconds.
N	- Number of integration in .01 seconds (rounded down)
C	- Damping coefficient, pounds-seconds per inch
FD	- Damped frequency, radians per second.
DEC	- Logarithmic decrement.
YY	- Yield deflection
J	- Counter for Nth. iteration interval (deflection storage).
JJ	- Counter
L	- Counter for storage interval.
LL	- Counter.
I	- Counter for number of the iteration interval.
VB	- Velocity at beginning of interval, inches per second.
YB	- Deflection at beginning of interval, inches.
YPE	- Plastic deflection at end of interval, inches.
PYE	- Plastic deflection during N intervals, inches.

YM	- Maximum deflection, inches.
TM	- Time of maximum deflection, seconds.
SD	- Summing variable for damped work.
CEI	- Summing variable for input work.
CEO	- Summing variable for output work.
T	- Time, seconds.
YE	- Deflection at end of interval, inches.
R	- Frame resistance, pounds.
F	- Impulse force, pounds.
YF	- Deflection at beginning of former interval, inches.
VF	- Velocity at beginning of former interval, inches per second.
AB	- Acceleration at beginning of interval, inches per second^2.
V( )	- Velocity at end of storage interval, inches per second.
A( )	- Acceleration at end of storage interval, inches per second^2.
D	- Damped work, pounds-inches.
W	- Input work, pounds-inches.
KE	- Kenetic energy, pounds-inches.
PE	- Potential energy, pounds-inches.
TE	- KE + PE, pounds-inches.
PW	- Plastic work, pounds-inches.
WN	- Net input work, pounds-inches.
YPB	- Plastic deflection at beginning of interval, inches.
Y( )	- Deflection at TT( ).
*YP( )	- Plastic deflection occuring during a previous interval of .01 seconds.
*PY( )	- Accumulated plastic deflection.
TT( )	- Time, seconds.

DUC - Ductility

* The value of YP( ) for the first interval is a better estimate of PY( ) , for the first interval as it is calculated from YY (occuring at any time) rather than the deflection at the beginning of the first plastic interval (which may exceed YY).

```
C
C
C        ELASTO-PLASTIC RESPONSE
C
C
      IMPLICIT REAL *8(A-H,K,M,O-Z)
      DIMENSION Y(200),YP(200),PY(200),TT(200),V(200),A(200)
C
C
C     INPUT AND DEFINING PARAMETERS
      DO 124 NFMS=1,32
      READ(5,13)FRM,IST,FI,TR,TI,K,Q,PD
   13 FORMAT(A1,I3,F15.5,2F10.9,2F10.4,F10.9)
      M=1.73D0
      DT=.0001D0
      WRITE(6,14)FRM,IST
   14 FORMAT('1','          ****************************************'/'
     1           RESPONSE ANALYSIS OF FRAME  ',A1,'  TEST ' ,I3,/'
     2   ****************************************'//)
      WRITE(6,16)M,K,PD,Q,DT
   16 FORMAT('    SINGLE D.O.F. IDEALIZATION - MASS = ',F6.4, ' LBS.SEC.S
     1EC/IN'/'                              STIFFNESS = ',F7.1, ' LBS/IN'/'
     2               RATIO OF CRITICAL DAMPING = ',F6.4, / '           MAXI
     3MUM FRAME RESISTANCE = ',F6.1,' LBS'/'      NUMERICAL INTEGRATION
     4INTERVAL = ',F7.5,' SEC')
      WRITE(6,15)FI,TR,TI
   15 FORMAT(//,'    TRIANGULAR FORCE PULSE - PEAK = ',F6.1,' LBS ' /'
     1                        RISE TIME = ',F6.4,' SEC   '  /'
     2          TOTAL TIME = ',F6.4,' SEC')
C
C     CALCULATION OF CONSTANTS AND INITIALIZING
C
      N=.01D0/DT+.5D0
      C=PD*2.0D0*DSQRT(M*K)
      B=C/(2.D0*M)
      FD=DSQRT(K/M-B**2)
      DEC=B*2.0D0*3.14159/FD
      YY=Q/K
      J=N
      JJ=N
      L=1
      LL=1
      I=1
      VB=0.0D0
      YB=0.D0
      YPE=0.D0
      PYE=0.0D0
      YM=0.D0
      TM=0.D0
      SD=0.0D0
      CEI=0.D0
      CEO=0.D0
      T=0.D0
C
C     CALCULATION OF DEFLECTION AT END OF FIRST INTERVAL
```

```
C
      YE=(FI/TR)*(DEXP( -B*DT)*(-((1.0D0/K+B*C/K**2)/FD)*DSIN(FD*DT)+(C/
     1K**2)*DCOS(FD*DT))-C/K**2+DT/K)
      IF(YE.LE.YY) GO TO 100
C
C     CALCULATION OF DEFLECTION AT END OF SUBSEQUENT INTERVALS
C
C     CHOICE OF FRAME RESISTANCE FORCE
C
  111 R=Q
  101 GO TO 102
  112 R=Q-K*(YM-YE)
      GO TO 102
  100 R=K*YE
  102 T=T+DT
C
C     CHOICE OF FORCING FUNCTION
C
      IF(T.GT.1.5)GO TO 103
      IF(T.GE.TR)GO TO 104
      F=(FI/TR)*T
      GO TO 107
  104 IF(T.LE.TI)GO TO 106
      F=0.D0
      GO TO 107
  106 F=FI*(1.D0-(T-TR)/(TI-TR))
  107 CONTINUE
C
C     ACCELERATION AND VELOCITY AT T  AND DISPLACEMENT AT T+DT
C
      YF=YB
      YB=YE
      VF=VB
      AB=(F-R-C*(YB-YF)/DT)/(M+C*DT/2.0D0)
      VB=(YB-YF)/DT+AB*DT/2.D0
      YE=2.D0*YB-YF+AB*DT**2
C     STORING VELOCITY AND ACCELERATION
      IF(I.NE.JJ)GO TO 121
      V(LL)=VB
      A(LL)=AB
      JJ=JJ+N
      LL=LL+1
  121 CONTINUE
C
C     ENERGY BALANCE AT END OF FORCE PULSE
C
      IF(TI-T-.01*DT)122,113,115
  122 IF(TI-T+.01*DT)114,113,113
C     WORK DISSIPATED BY DAMPING FORCE
  115 SD=SD+(VF+VB)**2
C     EXTERNAL WORK INPUT BY FORCE PULSE
      NY=(-1)**I
      IF(TR-T-.01*DT)123,117,116
  123 IF(TR-T+.01*DT)118,117,117
  116 IF(NY.EQ.1)GO TO 119
```

```
      CEI=CEI+4.D0*YB
      GO TO 114
  119 CEI=CEI+2.D0*YB
      GO TO 114
  117 CEI=CEI+YB
      CEO=YB
      GO TO 114
  118 IF(NY.EQ.1)GO TO 120
      CEO=CEO+4.D0*YB
      GO TO 114
  120 CEO=CEO+2.D0*YB
      GO TO 114
  113 D=-(C*DT/4.D0)*(SD+(VF+VB)**2)
      W=-((DT*FI/(TR*3.D0))*CEI+(DT*FI/((TR-TI)*3.D0))*(CEO+YB))
      KE=M*VB**2/2.0D0
      PE=K*(YB-YPE)**2/2.D0
      TE=KE+PE
      PW=-Q*YPE
      WN=W+D+PW
  114 CONTINUE
C
C     CALCULATION OF PLASTIC DEFORMATIONS
C
      YPB=YPE
C     IS THIS A PLASTIC OR AN ELASTIC INTERVAL ?
      IF(YM.LT.YY) GO TO 108
      IF(YE.LT.YM) GO TO 108
      YPE=YE-YY
      PYE=PYE+YE-YB
      GO TO 109
  108 YPE=YPB
  109 CONTINUE
C
C     STORING DEFLECTIONS
C
      I=I+1
      IF(I.NE.J) GO TO 105
      Y(L)=YE
      YP(L)=YPE
      PY(L)=PYE
      TT(L)=(DFLOAT(I))*DT
      L=L+1
      J=J+N
      PYE=0.0D0
  105 CONTINUE
C
C     DECIDE ON RESISTANCE FUNCTION FOR NEXT INTERVAL
C
      IF(YE.LT.YM) GO TO 110
      YM=YE
      TM=T
  110 IF(YM.LT.YY) GO TO 100
      IF(YE.LT.YM) GO TO 112
      GO TO 111
  103 CONTINUE
```

```
C
C     TYPING OUTPUT
C
      WRITE(6,7)
    7 FORMAT(//'     ENERGY BALANCE AT END OF FORCE PULSE (UNITS=LBS-IN)
     1',/)
      WRITE(6,8)W,KE
    8 FORMAT('     EXTERNAL WORK = ',F10.4,'    KINETIC ENERGY = ',F10.4)
      WRITE(6,9)D,PE
    9 FORMAT('       DAMPED WORK = ',F10.4,'  POTENTIAL ENERGY = ',F10.4)
      WRITE(6,10)PW
   10 FORMAT('      PLASTIC WORK = ',F10.4)
      WRITE(6,11)WN,TE
   11 FORMAT(/,'    NET INPUT WORK = ',F10.4,5X,' TOTAL ENERGY = ',F10.4)
      WRITE(6,5)YM,TM
    5 FORMAT(//,'    MAXIMUM DEFLECTION = ',F6.4,' INCHES AT TIME = ',F6.
     24,' SECONDS')
      DUC=YM/YY
      WRITE(6,17)YY,DUC
   17 FORMAT(/,'    YIELD DEFLECTION = ',F6.4,' INCHES   DUCTILITY (YM/YY
     1) = ',F5.2)
      WRITE(6,3)FD,DEC
    3 FORMAT(/,'    DAMPED FREQUENCY = ',F6.3,' RAD/SEC    LOG DECREMENT
     1= ',F6.4)
      WRITE(6,1)
    1 FORMAT(///  ,'                                     RESPONSE')
      WRITE(6,2)
    2 FORMAT(//,'          T         Y(T)       YP(T)      PY(T)        V(T)
     1  A(T)',/)
      WRITE(6,12)
   12 FORMAT('        SEC          IN          IN          IN       IN/SEC    IN/S
     1EC/SEC')
      WRITE(6,6)
    6 FORMAT('     0.00        0.00        0.00        0.00        0.00          0
     1.00')
      WRITE(6,4)(TT(I),Y(I),YP(I),PY(I),V(I),A(I),I=1,150)
    4 FORMAT(' ',4F10.5,F11.5,F12.5)
  124 CONTINUE
      STOP
      END
```

****

RESPONSE ANALYSIS OF FRAME 3 TEST 6

****

```
SINGLE D.O.F. IDEALIZATION - MASS = 1.7300 LBS.SEC.SEC/IN
                           STIFFNESS = 10300.0 LBS/IN
        RATIO OF CRITICAL DAMPING = 0.0290
         MAXIMUM FRAME RESISTANCE = 1100.0 LBS
   NUMERICAL INTEGRATION INTERVAL = 0.00010 SEC


TRIANGULAR FORCE PULSE - PEAK = 1210.0 LBS
                    RISE TIME = 0.0900 SEC
                   TOTAL TIME = 0.1950 SEC


  ENERGY BALANCE AT END OF FORCE PULSE (UNITS=LBS-IN)

 EXTERNAL WORK =     20.8509    KINETIC ENERGY =      0.0162
   DAMPED WORK =     -3.1402  POTENTIAL ENERGY =      0.8932
  PLASTIC WORK =    -16.8014

NET INPUT WORK =      0.9094      TOTAL ENERGY =      0.9094


MAXIMUM DEFLECTION = 0.1221 INCHES AT TIME = 0.1141 SECONDS

YIELD DEFLECTION = 0.1068 INCHES   DUCTILITY (YM/YY) =  1.14

DAMPED FREQUENCY = 77.128 RAD/SEC    LOG DECREMENT = 0.1823
```

RESPONSE

T	Y(T)	YP(T)	PY(T)	V(T)	A(T)
SEC	IN	IN	IN	IN/SEC	IN/SEC/SEC
0.00	0.00	0.00	0.00	0.00	0.00
0.01000	0.00120	0.0	0.0	0.36129	68.92473
0.02000	0.00895	0.0	0.0	1.23386	95.63449
0.03000	0.02588	0.0	0.0	2.10731	63.60250
0.04000	0.04946	0.0	0.0	2.49896	5.19852
0.05000	0.07356	0.0	0.0	2.21178	-59.26635
0.06000	0.09203	0.0	0.0	1.43503	-83.08026
0.07000	0.10213	0.0	0.0	0.62041	-66.84258
0.08000	0.10585	0.0	0.0	0.22081	-9.50811
0.09000	0.10870	0.00190	0.00190	0.46751	61.49155
0.10000	0.11531	0.00851	0.00661	0.74073	-6.34279
0.11000	0.12130	0.01451	0.00600	0.35055	-71.20825
0.12000	0.12023	0.01527	0.00077	-0.65327	-122.39249
0.13000	0.10752	0.01527	0.0	-1.85484	-107.39127
0.14000	0.08453	0.01527	0.0	-2.61014	-34.26024
0.15000	0.05824	0.01527	0.0	-2.40577	55.12608
0.16000	0.03717	0.01527	0.0	-1.62501	110.06415
0.17000	0.02656	0.01527	0.0	-0.51104	101.62966
0.18000	0.02563	0.01527	0.0	0.21750	37.25635
0.19000	0.02828	0.01527	0.0	0.17303	-41.92024
0.20000	0.02532	0.01527	0.0	-0.50220	-6[illegible].50768

0.21000	0.01916	0.01527	0.0	-0.94978	-13.88954
0.22000	0.00968	0.01527	0.0	-0.85166	37.10422
0.23000	0.00372	0.01527	0.0	-0.28607	70.09410
0.24000	0.00441	0.01527	0.0	0.41323	62.81273
0.25000	0.01110	0.01527	0.0	0.85302	21.05603
0.26000	0.01980	0.01527	0.0	0.80105	-39.53675
0.27000	0.02562	0.01527	0.0	0.30763	-62.95619
0.28000	0.02545	0.01527	0.0	-0.33461	-59.08327
0.29000	0.01965	0.01527	0.0	-0.76338	-22.65171
0.30000	0.01168	0.01527	0.0	-0.75953	24.73289
0.31000	0.00605	0.01527	0.0	-0.32250	56.34328
0.32000	0.00578	0.01527	0.0	0.26544	55.35982
0.33000	0.01077	0.01527	0.0	0.68061	23.75380
0.34000	0.01804	0.01527	0.0	0.70060	-19.62693
0.35000	0.02346	0.01527	0.0	0.33162	-50.23705
0.36000	0.02411	0.01527	0.0	-0.20490	-51.67953
0.37000	0.01983	0.01527	0.0	-0.60444	-24.43191
0.38000	0.01322	0.01527	0.0	-0.65167	15.15681
0.39000	0.00803	0.01527	0.0	-0.33586	44.61702
0.40000	0.00709	0.01527	0.0	0.15218	48.07304
0.41000	0.01072	0.01527	0.0	0.53456	24.74859
0.42000	0.01671	0.01527	0.0	0.60409	-11.26408
0.43000	0.02165	0.01527	0.0	0.33596	-39.46106
0.44000	0.02284	0.01527	0.0	-0.10654	-44.56520
0.45000	0.01979	0.01527	0.0	-0.47065	-24.75983
0.46000	0.01437	0.01527	0.0	-0.55312	7.89400
0.47000	0.00969	0.01527	0.0	-0.33260	34.74594
0.48000	0.00831	0.01527	0.0	0.06729	41.17576
0.49000	0.01035	0.01527	0.0	0.41240	24.51558
0.50000	0.01573	0.01527	0.0	0.51397	-4.99542
0.51000	0.02014	0.01527	0.0	0.32639	-30.44770
0.52000	0.02167	0.01527	0.0	-0.03378	-37.92006
0.53000	0.01959	0.01527	0.0	-0.35948	-24.06022
0.54000	0.01521	0.01527	0.0	-0.47179	2.52076
0.55000	0.01105	0.01527	0.0	-0.31785	26.54205
0.56000	0.00942	0.01527	0.0	0.00542	34.30951
0.57000	0.01110	0.01527	0.0	0.31154	23.43302
0.58000	0.01502	0.01527	0.0	0.43159	-0.42588
0.59000	0.01891	0.01527	0.0	0.30745	-23.00464
0.60000	0.02061	0.01527	0.0	0.01835	-31.85220
0.61000	0.01928	0.01527	0.0	-0.26327	-22.66856
0.62000	0.01579	0.01527	0.0	-0.39374	-1.33000
0.63000	0.01217	0.01527	0.0	-0.29561	17.81137
0.64000	0.01042	0.01527	0.0	-0.03303	24.05330
0.65000	0.01144	0.01527	0.0	0.22934	21.79717
0.66000	0.01454	0.01527	0.0	0.35798	2.79446
0.67000	0.01791	0.01527	0.0	0.28268	-16.93853
0.68000	0.01967	0.01527	0.0	0.05410	-26.41552
0.69000	0.01832	0.01527	0.0	-0.19445	-20.84531
0.70000	0.01618	0.01527	0.0	-0.32441	-3.97290
0.71000	0.01306	0.01527	0.0	-0.26398	14.36705
0.72000	0.01130	0.01527	0.0	-0.06698	23.33949
0.73000	0.01182	0.01527	0.0	0.15328	19.83592
0.74000	0.01423	0.01527	0.0	0.23302	4.92421
0.75000	0.01711	0.01527	0.0	0.23476	-12.06255
0.76000	0.01885	0.01527	0.0	0.07705	-21.62402
0.77000	0.01853	0.01527	0.0	-0.13555	-15.78677
0.78000	0.01642	0.01527	0.0	-0.26377	-5.65990
0.79000	0.01377	0.01527	0.0	-0.24027	10.01555
0.80000	0.01207	0.01527	0.0	-0.09472	19.35656

0.81000	0.01221	0.01527	0.0	0.11097	17.72078
0.82000	0.01405	0.01527	0.0	0.23661	6.23528
0.83000	0.01648	0.01527	0.0	0.22569	-8.20145
0.84000	0.01814	0.01527	0.0	0.09022	-17.46330
0.85000	0.01814	0.01527	0.0	-0.08929	-16.64629
0.86000	0.01655	0.01527	0.0	-0.21148	-5.64412
0.87000	0.01432	0.01527	0.0	-0.21118	6.60068
0.88000	0.01272	0.01527	0.0	-0.09391	15.60947
0.89000	0.01260	0.01527	0.0	0.07025	15.57739
0.90000	0.01397	0.01527	0.0	0.18831	6.91789
0.91000	0.01600	0.01527	0.0	0.19689	-5.19466
0.92000	0.01754	0.01527	0.0	0.09604	-13.89960
0.93000	0.01775	0.01527	0.0	-0.05360	-14.52411
0.94000	0.01659	0.01527	0.0	-0.16700	-7.07591
0.95000	0.01475	0.01527	0.0	-0.19293	3.96588
0.96000	0.01328	0.01527	0.0	-0.09683	12.32758
0.97000	0.01298	0.01527	0.0	0.03914	13.49467
0.98000	0.01396	0.01527	0.0	0.14748	7.13555
0.99000	0.01563	0.01527	0.0	0.16938	-2.89787
1.00000	0.01703	0.01527	0.0	0.09650	-10.88694
1.01000	0.01739	0.01527	0.0	-0.02664	-12.49572
1.02000	0.01657	0.01527	0.0	-0.12964	-7.11231
1.03000	0.01506	0.01527	0.0	-0.15632	1.97523
1.04000	0.01374	0.01527	0.0	-0.09524	9.57090
1.05000	0.01333	0.01527	0.0	0.01592	11.53250
1.06000	0.01401	0.01527	0.0	0.11340	7.02002
1.07000	0.01536	0.01527	0.0	0.14379	-1.18358
1.08000	0.01661	0.01527	0.0	0.09320	-8.37251
1.09000	0.01706	0.01527	0.0	-0.00680	-10.60900
1.10000	0.01650	0.01527	0.0	-0.09866	-6.87094
1.11000	0.01529	0.01527	0.0	-0.13185	0.50956
1.12000	0.01412	0.01527	0.0	-0.09955	7.28478
1.13000	0.01364	0.01527	0.0	-0.00090	9.72819
1.14000	0.01409	0.01527	0.0	0.08532	5.67591
1.15000	0.01517	0.01527	0.0	0.12051	0.05921
1.16000	0.01627	0.01527	0.0	0.08740	-6.30070
1.17000	0.01676	0.01527	0.0	0.00733	-8.99209
1.18000	0.01641	0.01527	0.0	-0.07330	-6.44445
1.19000	0.01545	0.01527	0.0	-0.10980	-0.53414
1.20000	0.01443	0.01527	0.0	-0.03388	5.41337
1.21000	0.01332	0.01527	0.0	-0.01263	8.10194
1.22000	0.01419	0.01527	0.0	0.06250	6.18491
1.23000	0.01504	0.01527	0.0	0.09972	0.92576
1.24000	0.01599	0.01527	0.0	0.08007	-4.61602
1.25000	0.01659	0.01527	0.0	0.01693	-7.35830
1.26000	0.01631	0.01527	0.0	-0.05282	-5.30456
1.27000	0.01555	0.01527	0.0	-0.09025	-1.24371
1.28000	0.01468	0.01527	0.0	-0.07507	3.90208
1.29000	0.01417	0.01527	0.0	-0.02235	5.56116
1.30000	0.01430	0.01527	0.0	0.04420	5.60966
1.31000	0.01436	0.01527	0.0	0.08144	1.49680
1.32000	0.01577	0.01527	0.0	0.07194	-3.26517
1.33000	0.01627	0.01527	0.0	0.02301	-6.01005
1.34000	0.01619	0.01527	0.0	-0.03653	-5.30563
1.35000	0.01561	0.01527	0.0	-0.07322	-1.69708
1.36000	0.01487	0.01527	0.0	-0.06775	2.69921
1.37000	0.01432	0.01527	0.0	-0.02499	5.40409
1.38000	0.01441	0.01527	0.0	0.02974	4.99709
1.39000	0.01492	0.01527	0.0	0.06561	1.33984
1.40000	0.01550	0.01527	0.0	0.06355	-2.19837